Master's thesis

NTNU
Norwegian University of Science and Technology
Faculty of Information Technology and Electrical Engineering
Department of Electric Power Engineering

Erlend Vabø

Electric water heaters as flexible energy resources in the power grid

Master's thesis in Energy and Environmental Engineering
Supervisor: Jayaprakash Rajasekharan
Co-supervisor: Surya Venkatesh Pandiyan
June 2023

NTNU
Norwegian University of
Science and Technology

Erlend Vabø

Electric water heaters as flexible energy resources in the power grid

Master's thesis in Energy and Environmental Engineering
Supervisor: Jayaprakash Rajasekharan
Co-supervisor: Surya Venkatesh Pandiyan
June 2023

Norwegian University of Science and Technology
Faculty of Information Technology and Electrical Engineering
Department of Electric Power Engineering

NTNU
Norwegian University of
Science and Technology

Summary

The intermittency of renewable power generation from wind and solar is challenging as it can cause severe issues for grid safety and reliability. Demand-side flexibility (DSF) from aggregated electric water heaters (EWHs) is a promising solution to mitigate this challenge, as the load of residential EWHs can be shifted to periods with a high share of renewable generation present to supply the load. However, as good business cases still need to be improved for aggregators with EWHs, this work investigates how aggregators can maximise flexibility from EWHs.

A review of previous work assesses three pillars for aggregators with EWHs; modelling of EWHs, market participation with EWHs and other flexible resources, and optimisation problems concerning EWHs. The review indicates significant differences in modelling accuracy, setups for market participation and optimisation techniques applied in problems with EWHs. It is also evident that many technical challenges and barriers must be overcome for aggregators to control and optimise EWHs to achieve significant flexibility. One of the major challenges is to model the non-linear temperature dynamics of the EWHs accurately and computationally efficiently, which is essential to extract the maximum amount of flexibility with a low risk of cold water for consumers.

This work aims to find the best trade-off between the amount of flexibility, accuracy in modelling and computational efficiency for an optimisation problem created from scratch with aggregated residential EWHs. A 10-layer stratified temperature model with a one-minute resolution is used for up to 100 EWHs, assumed to be part of a portfolio of flexible resources applied in a balancing market. A genetic algorithm (GA) maximises flexibility and, coincidently, revenue from the EWHs, and handles the non-linear EWH temperature model with high accuracy. Additionally, three different reconnection strategies are applied to manage the aggregated load of many EWHs connected to the grid simultaneously.

The results indicate that aggregators can provide up to 5.8 kWh of flexibility per EWH per day using the GA. This can translate to revenue of up to 1.5 EUR per day per EWH when applying prices from manual frequency restoration reserve (mFRR) markets of January 2023. The GA performs well for providing a high amount of flexibility, modelling accurately and being computationally manageable for a low number of EWHs. However, its simulation time scales poorly with many aggregated EWHs in the portfolio. In comparison, the simulation time of a simplified reference algorithm scales linearly with the number of EWHs and can therefore be useful for aggregators with a high number of EWHs in their portfolio.

The results also indicate that it is possible to apply the reconnection strategies without negatively affecting flexibility or peak load. All of the reconnection strategies implemented in the simulations resulted in higher or equal average flexibility than those without reconnection strategies. Additionally, two reconnection strategies significantly reduced peak load compared to the simulations without reconnection strategies.

Sammendrag

Usammenhengende kraftproduksjon fra vind- og solenergi kan være utfordrende for strømnettet. Forbrukerfleksibilitet fra aggregerte elektriske varmtvannsberedere er en lovende løsning for å håndtere denne utfordringen, ettersom varmtvannsberedere hos forbrukere kan skifte forbruk til perioder med høy andel fornybar kraftproduksjon. Ettersom det behøves bedre forretningsmodeller for aggregatorer med varmtvannsberedere, undersøker dette arbeidet hvordan aggregatorer kan maksimere forbrukerfleksibilitet fra aggregerte varmtvannsberedere.

En oversikt over tidligere forskningsarbeid vurderer tre hovedtemaer for aggregatorer med varmtvannsberedere. Det første temaet er modellering av berederne, det andre deltakelse i markeder med beredere og andre fleksible ressurser, og det tredje er optimeringsproblemer knyttet til beredere. Oversikten viser betydelige forskjeller i modelleringsnøyaktighet, oppsett for markedsdeltagelse og bruk av optimeringsmetoder. Det kommer også frem at mange tekniske utfordringer må løses og barrierer må brytes for at aggregatorer i større grad skal kunne kontrollere og optimere varmtvannsberedere til forbrukere for å oppnå en betydelig mengde fleksibilitet. En av de største utfordringene er å modellere beredernes ikke-lineære temperaturdynamikk nøyaktig og med lav kjøretid, som er avgjørende for å få ut mest mulig fleksibilitet med lav risiko for kaldt vann hos forbrukerne.

Denne masteroppgaven tar sikte på å finne den beste avveiningen mellom mengden fleksibilitet, nøyaktighet i modellering og lavest mulig kjøretid til algoritmene for et problem laget fra bunnen som maksimerer fleksibilitet fra varmtvannsberedere. En modell med ti temperaturlag og ett minutts tidsoppløsning brukes for å nøyaktig modellere opptil 100 beredere. Deretter antas det at berederne gir fleksibilitet ved å delta i et nordisk balansemarked. For å maksimere fleksibiliteten og dermed inntektene for aggregatoren, brukes en genetisk algoritme for å håndtere beredernes ikke-lineære temperaturdynamikk med høy nøyaktighet innenfor en rimelig kjøretid. Deretter blir det benyttet tre ulike gjentilkoblingsstrategier for å håndtere situasjoner der mange beredere er tilkoblet nettet samtidig, som kan ha negative konsekvenser for nettet.

Resultatene viser at aggregatorer kan forvente å oppnå en energimengde p a opptil 5.8 kWh med fleksibilitet per bereder per dag. Dersom denne fleksibiliteten anvendes på balansemarkedet kan aggregatorer forvente å få en inntekt fra markedet på opptil 1.5 EUR per bereder per dag, med balansemarkedspriser fra januar 2023. Mens den genetiske algoritmen fungerer bra for å gi mye fleksibilitet, modellere nøyaktig og ha en brukbar kjøretid for et lavt antall beredere, skalerer kjøretiden dårlig for en portefølje med mange beredere. Til sammenligning skalerer en forenklet referansealgoritme lineært med antall beredere og kan derfor være bedre egnet for en portefølje med et høyt antall beredere.

Resultatene indikerer også at gjentilkoblingsstrategiene ikke påvirker mengden fleksibilitet eller den aggregerte topplasten til berederne på en negativ måte. Alle gjentilkoblingsstrategiene implementert i simuleringene resulterte i høyere eller lik gjennomsnittlig fleksibilitet sammenlignet med simuleringene uten gjentilkoblingsstrategi. I tillegg viste to av gjentilkoblingsstrategiene en betydelig reduksjon i aggregert topplast sammenlignet med simuleringene uten gjentilkoblingsstrategier.

Table of Contents

List of Tables

List of Figures

Preface

This thesis is submitted as part of the TET4900 - Electric Energy and Energy Systems course, as a master's thesis at NTNU in the spring of 2023. It builds upon my specialisation project, completed in the fall of 2022 [1]. I extend my heartfelt gratitude to my supervisor, Associate Professor Jayaprakash Rajasekharan, for his invaluable guidance and feedback throughout this process. I am also grateful to my co-supervisor, PhD Candidate Surya Venkatesh Pandiyan, for his contributions and opinions which have greatly influenced the work of this thesis. At last, I want to thank my girlfriend Ingvild for her love and support throughout the process of writing this thesis.

Abbreviations

AMI = advanced metering infrastructure

BRP = balance responsible party

DER = distributed energy resource

DSF = demand-side flexibility

DSO = distribution system operator

DP = dynamic programming

ENTSO-E = European Network of Transmission System Operators

EV = electric vehicle

EWH = electric water heater

FCR = frequency containment reserves

FMO = flexibility market operator

FO = flexibility operator

FRR = frequency restoration reserve

GA = genetic algorithm

IA = independent aggregator

ICT = information and communications technology

LP = linear programming

mFRR = manual frequency restoration reserve

MILP = mixed-integer linear programming

MPC = model predictive control

NVE = The Norwegian Water Resources and Energy Directorate

PSO = particle swarm optimisation

SA = simulated annealing

TS = tabu search

TSO = transmission system operator

1 Introduction

1.1 Background

In accordance with the Paris Agreement, the effects of climate change can be reduced by increasing the share of renewable energy production [2]. However, the intermittent nature of solar and wind power can cause issues for grid operators, such as voltage instabilities and congestion. While grid enforcement has traditionally been the solution to many problems in the grid, the European Green Deal has recently highlighted "flexibility" in the energy system as an essential solution and part of the future power grid [3].

Flexibility refers to changing power production or consumption in response to a signal to provide a grid service [4]. Demand-side flexibility (DSF) is particularly promising, as consumers can shift energy consumption to periods with more renewable production. Additionally, DSF can lead to lower and less volatile electricity prices for consumers [5].

On the demand side, the Nordic region is characterised by high electrification, including the widespread use of electric vehicles (EVs) and heating systems, where residential thermal power consumption significantly contributes to the total electricity consumption. As a result, thermal residential resources have a high potential to provide DSF in the Nordic region [5]. In Norway, the transmission system operator (TSO) has recently facilitated flexibility from thermal resources by making changes to the balancing markets [6].

1.2 Motivation

Residential electric water heaters (EWHs) are excellent thermal resources for flexibility as they have been estimated to have a flexibility potential of 600 MWh/h in the morning hours in Norway [7]. In February 2023, on behalf of the Norwegian government, The Energy Commission emphasised the importance of shifting load from EWHs away from the hours with peak load, indicating a political will to facilitate flexibility from EWHs [8].

EWHs have many advantages compared to other flexible resources. They have high theoretical flexibility potential, with estimates of 120 GWh or 20 GW daily in the EU [9]. EWHs also have high availability, are continuous in operation, have easy access to control and can store heat energy for a long time [10], [11].

From the grid perspective, load from EWHs contributes significantly to the peak load, as it is highly correlated with other loads [11]. Shifting the load from peak hours is not only beneficial for the grid but often also for consumers because of lower electricity prices and tariffs. Therefore, the objective in most literature on flexibility from EWHs is minimising electricity costs for consumers by load shifting.

In 2023, the European Network of Transmission System Operators (ENTSO-E) suggested that investments in flexible resources, like EWHs, must accelerate [12]. When many flexibility resources like EWHs are available, they can be aggregated and applied in balancing markets, for example, manual frequency restoration reserve (mFRR) markets [13]. Aggregating many EWHs is beneficial as it can simplify control algorithms and contribute better to achieving bids above the minimum bid size in markets [14].

Entities that can aggregate flexible assets and offer flexibility in electricity markets, directly or through a third party, are referred to as flexibility aggregators [15]. The aggregators must overcome many barriers and technical challenges to deliver flexibility into the markets, particularly within regulation, grid-wise and related to consumers. Another significant challenge is the non-linear temperature model of the EWHs, making it computationally challenging to perform optimisation of the EWHs. By modelling the temperature dynamics non-linearly using a stratified temperature model, aggregators can extract more flexibility with higher accuracy. Still, they must find good algorithms to deal with the computational complexity of this modelling.

1.3 Problem statement

This work investigates the research question of how aggregators can maximise flexibility from a group of residential EWHs using a non-linear accurate stratified temperature model. It is assumed that an aggregator applies flexibility as bids in an mFRR-market using a genetic algorithm (GA). In addition to flexibility maximisation, this work applies three reconnection strategies to avoid simultaneous reconnection and manage the peak load from the EWHs. At last, it is applied mFRR-prices, identifying potential market revenue from the flexible energy of EWHs.

1.4 Contributions

This work aims to contribute with the following to relevant scientific communities:

- Present an optimisation problem to maximise flexibility from residential EWHs.
- Develop a GA and a reference algorithm from scratch to solve the optimisation problem and apply reconnection strategies to the problem.
- Solve the optimisation problem with 24 use cases, asses the flexibility that can be provided for aggregators with EWHs for these use cases, and evaluate the trade-off between flexibility from the EWHs and the computational efficiency and accuracy of the algorithms.

1.5 Outline

This work consists of nine chapters. Chapter 2 explains relevant theory on EWHs, flexibility, aggregators, electricity markets and techniques to solve optimisation problems with EWHs. Then, Chapter 3 presents a literature review on modelling EWHs, market participation for aggregators and optimisation techniques relevant to problems with EWHs. Chapter 4 is a comprehensive chapter on the methodology explaining the research problem of this work, while Chapter 5 presents the case study to which the research problem is applied. Then, Chapter 6 presents a selection of the results from the case study, with a discussion in Chapter 7. Finally, Chapters 8 and 9 provide a conclusion and suggestions for future work.

2 Theory

The theory chapter is divided into three sections. Section 2.1 covers the design, operation, functionalities and modelling of EWHs, thereunder the single-zone and stratified models. Section 2.2 covers essential theoretical aspects of flexibility and market participation for aggregators, and lastly, suitable optimisation methods for optimisation problems relevant to EWH-aggregators are presented in Section 2.3. It can be noted that Section 2.1 and Section 2.2 are based on the specialisation project for this master's thesis, with additional input on the stratified models in Section 2.1 [1].

2.1 Electric water heaters (EWHs)

This section first presents the design, operation, and functionalities of EWHs. Then, the two popular types of EWH models, the single-zone and the stratified models, are described with mathematical modelling, typical values of parameters and how the parameters can be estimated, and the advantages and disadvantages of the two models. For simplicity and computational efficiency, it can be assumed that the temperature in the tank is uniform. Therefore, the EWH can be represented as one thermal zone, and this type of modelling is known as single-zone modelling. However, the single-zone temperature model does not accurately represent the temperature dynamics of the EWHs. The tank can instead be divided into multiple zones or layers, and this type of modelling is also known as multi-zone or multi-layer [16].

2.1.1 Design, operation, and functionalities

A traditional EWH consists of a water inlet, water outlet, thermostat, isolated top cover, one or multiple heating elements and mixing-, pressure relief- and safety valves [17]. A model of OSO Hotwaters SAGA-series S 300-product with this content is depicted in Figure 1. Most EWHs have one resistive heating element with negligible losses. The EWHs work by hot water being drawn through the water outlet at a temperature T_{out} while cold water comes in through the water inlet at T_{in}. Combined with constant heat losses to the environment, this leads to an overall loss of temperature and energy in the tank. When consumers use a significant amount of hot water, or it has passed a long enough time since the last heating process occurred, the temperature registered by the thermostat will go below a specific temperature, T_{low}, initiating a new heating process. The heating element then supplies the EWH with constant power until the thermostat registers the temperature T_{high}. The set point for T_{high} is 75 °C, with T_{low} being a few degrees lower for most products in the Norwegian market [18]. However, the temperatures are significantly lower in most other countries, as the Norwegian heaters are typically made of stainless steel that can handle higher temperatures [19]. The set-point temperatures are high enough to ensure consumers hot water and avoid the risk of developing the legionella bacteria, but not too high as heating losses to the environment increase with temperature.

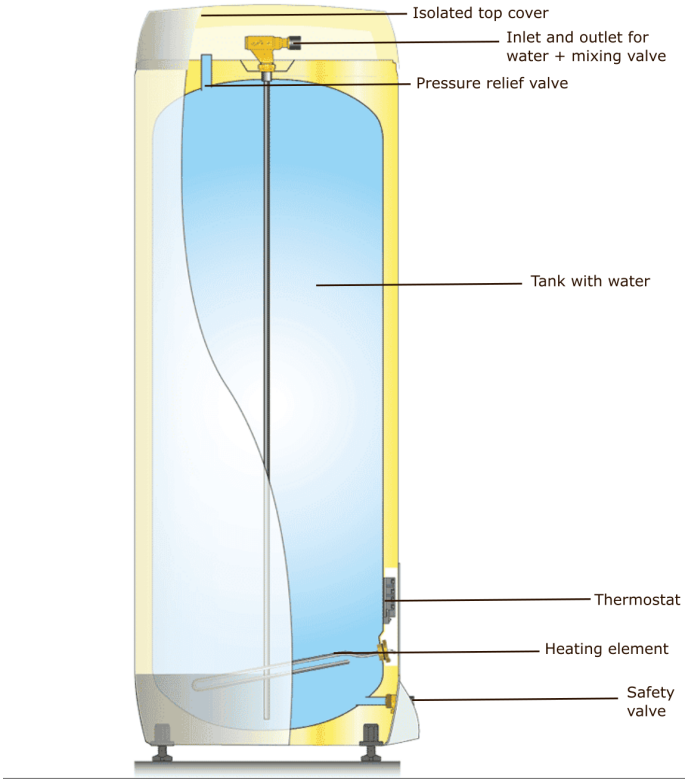

Figure 1: A model of the EWH SAGA S 300 from OSO Hotwater with its components, taken from [1] based on [17]

Some new products, like OSO Charge, have smart features [20]. This smartness can be a part of a new EWH or an extension of existing products. The smart features can include temperature sensors and voltage, current, and frequency measurements at a high sampling rate. Although EWHs with these smart systems typically cost 10-20% more than regular EWHs, it is facilitated in Norway as ENOVA supports the purchase of such smart water heaters with 5000 NOK [9], [21]. Smart EWHs can be controlled with a scheduling plan based on electricity prices to save electricity costs. Additionally, controlling EWHs based on voltage in the local grids has been proven successful in pilots [22]. However, despite the many advantages, smart EWHs are still not implemented on a large scale. A cheaper and more mature alternative is to control existing EWHs with a plug capable of overriding the thermostat [23].

2.1.2 Single-zone model: energy balance and parameters

In the single-zone model, the physical energy balance of an EWH can be modelled as a first-order differential equation, with the state variable for temperature above the thermostat, T [15]. The temperature gradient $\frac{dT}{dt}$ can then be modelled as proportional to the energy delivered by the heating element, Q_H, the energy lost by water withdrawal, Q_{flow}, and heat loss due to differences in temperature in the tank and ambient surroundings, Q_{loss}. This energy balance is illustrated in Figure 2 and shown in equation (1), where C_p is the heat capacity of the hot water tank. The equation can be written in more detail as in Equation (2). Further, Table 1 presents the parameters represented with typical values and an estimate of uncertainty level, and the sources and assumptions for the typical values and uncertainty levels. The main drawback of the single-zone model is that it inaccurately represents the temperature dynamics of the EWH.

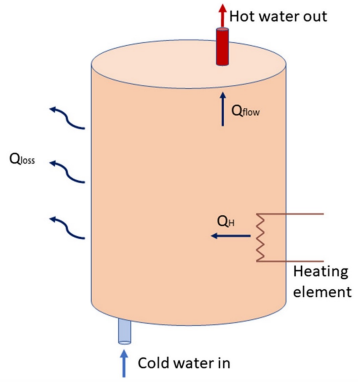

Figure 2: Energy balance in a single-zone temperature modelled EWH with one heating element [24]

$$Cp * \frac{dT}{dt} = Q_{flow} + Q_{loss} + Q_H \tag{1}$$

$$Cp * \frac{dT}{dt} = \rho * W_r * c_p * (T_{in} - T) + G * (T_{amb} - T) + Q_H \tag{2}$$

Table 1: Parameters used for modelling EWHs, including typical values and estimating the uncertainty level of the parameters. Additionally, it is presented the source of information and the assumptions for the typical values and uncertainty

Symbol	**Name**	**Typical value**	**Unit**	**Uncertainty level of parameter**	**Ref.**	**Assumptions**
ρ	Water density	997	kg/m^3	Low	[25]	Based on T_{amb}
c_p	Specific heat capacity of water	4186	J/kg°C	Low	[26]	-
T_{amb}	Ambient temperature	24	°C	Medium	[18]	Norwegian conditions
T_{in}	Inlet temperature	10	°C	Medium	[27]	-
V	Volume of tank	200	L	High	[17]	-
C_p	Heat capacity of the EWH	8.44·10^5	J/°C	High	-	$C_p = c_p * \rho * V$
G	Heat loss coefficient	1.36	W/°C	High	[17]	Corresponding to a rated heat loss of 66 W
Q_H	Heating element of the EWH	2000	W	High	[17]	-
Wr	Water drawn per time instant	0-0.20	L/s	Very high	[28]	Typical value for a shower is 0.20 L/s

Most parameters are, to some degree, uncertain. Hot water usage is classified as very uncertain, as it includes many different applications like showers, bathing, food preparation, hand washing, dishwashers, and washing machines [29]. As the parameters are uncertain, they must be estimated in a sufficiently accurate way to optimise flexibility from the EWHs.

2.1.3 Stratified models: extending the energy balance equation

The main reason there are temperature differences in the tank is that when hot water is drawn from the top, cold water replaces it at the bottom. As a result, there is often a clear physical separation of cold and hot water in the tank called the thermocline [30]. This separation is usually below the heating element, and when hot water is drawn at the top, the thermocline moves upwards, approaching and often triggering the thermostat. In some cases, it also passes the height of the thermostat. Other reasons for temperature differences are convection, heating of the water near the heating element, and differences in water density. With multiple withdrawals of hot water, the physical processes create varying temperatures in the tank, from cold at the bottom to hot at the top.

In contrast, several physical processes work against stratification [31]. First, de-stratification due to heat losses is based on Newton's cooling law, stating that the heat losses are higher where the temperature is higher [32]. Secondly, conduction occurs between water of different temperatures and between water and the tank's walls. Lastly, there is buoyancy in the water when the tank's heating element is placed such that the water temperature is higher near the heating element than above [33].

Thermal zones or mathematical layers can model the temperature differences in the EWHs. While the representation of thermal zones is based on physics, the mathematical layers, denoted as l, can represent one of N perfectly mixed layers of equal volume, V_l. Further, $Q_{flow,l}$ and $Q_{loss,l}$ can represent energy flow and heating loss in each layer, while $Q_{H,l}$ and $Q_{conv,l}$ can represent added energy from the heating element and convection in each layer, respectively. Using this notation, the layers with heating elements will rapidly increase in temperature when the EWH is turned on. It can be assumed that the temperatures in each layer above the heating element achieve a temperature equal to the average temperature of the considered layers to capture the buoyancy effect [34]. This non-linear effect can be represented as $Q_{buoyancy,l}$ [34].

To represent the multi-layer model mathematically, equation (1) can be extended to equation (3), with $Q_{conv,l}$ given values as in Table 2. K_l is the conductivity coefficient between the layers, found to have a typical dimensionless value of 2.21 using 10 layers [33]. With the use of Q_{flow}, Q_{conv} and Q_{env} to represent energy flow, convection and heating losses to the environment, and two heating elements to provide Q_H, Figure 3 illustrates the energy balance in a stratified 10-layer model [33].

$$Cp * \frac{dT_l}{dt} = Q_{flow,l} + Q_{loss,l} + Q_{H,l} + Q_{conv,l} + Q_{buoyancy,l} \tag{3}$$

Table 2: Representation of the added energy for a layer due to convection for the different layers

Layer	**Q_conv, l**
Bottom layer	$K_l * (T_{l+1} - T_l)$
All layers between bottom and top	$K_l * (T_{l+1} + T_{l-1} - 2 * T_l)$
Top layer	$K_l * (T_{l-1} - T_l)$

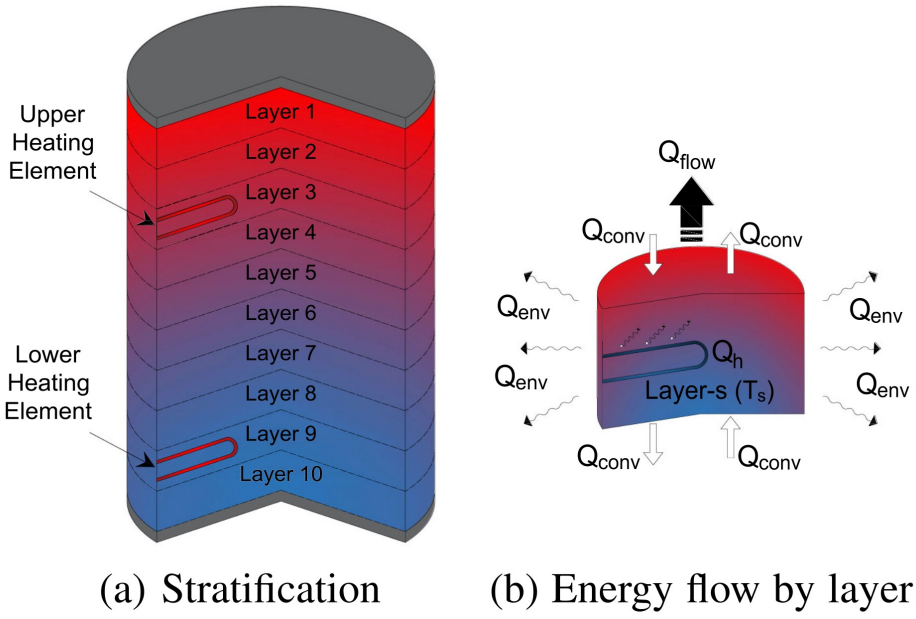

Figure 3: Energy balance in a stratified 10-layer model with two heating elements [33]

2.2 Market participation with flexible resources

This section presents how EWHs can be applied as flexible resources in markets. As aggregators are essential to delivering flexibility, the concepts of flexibility and the role of aggregators are first defined. Then, market participation relevant to the flexibility aggregators is presented, emphasising flexibility markets and balancing markets in the Nordics.

2.2.1 Flexibility

Flexibility can be defined as changing the production or consumption of power in response to a signal to deliver a grid service [4]. There are several drivers for flexibility, which can be differentiated between the production-based, grid-based, and demand-based drivers. On the production side, a significant concern is that renewable energy generation from wind and solar is intermittent and uncertain. From the grid operator's perspective, this contributes to power imbalances and frequency deviations. The grid operators are also concerned with voltage fluctuations, congestion and bidirectional power flows, which can be handled by flexible energy to some extent. On the demand side, flexibility is largely driven by advancements in metering, information- and communication technologies (ICT), and active consumer behaviour.

Different flexibility services can be provided primarily to DSOs and TSOs, but also to balance responsible parties (BRPs) and prosumers. The Norwegian Water Resources and Energy Directorate (NVE) distinguishes three flexibility services in the distribution grid, which are all relevant to the DSOs [9]. These are voltage control, grid capacity management, and congestion management. The gains of these services for the DSOs can be to delay or avoid investments in the grid, optimise asset use and reduce grid losses. For TSOs, to avoid grid problems like blackouts, it is essential to maintain the balance of the power system. In practice, this is done by control actions to keep the frequency near the set point of 50 Hz.

There are many ways to characterise flexible resources. The flexible resources can be characterised by their parameters, which can be defined as power, reaction duration, ramping capacity, up-, and down-ramping rates, direction, service duration, energy capacity, recovery duration, and rebound effect [35]. In this context, the rebound effect refers to turning many applications on simultaneously after being turned off earlier. Moreover, EWHs have high energy capacity and thermal

inertia between T_{high} and T_{low}, allowing them to provide a significant amount of power with a long service duration [18]. As EWHs are curtailable, they can delay heating in periods with high load and shift it to periods with lower stress on the grid. Crucially, this is possible without negatively affecting user temperature comfort or creating significant rebounds [7]. Therefore, EWHs are well suited to deliver flexibility by shifting load or delivering frequency response by frequency containment reserves (FCR) or frequency restoration reserves (FRR) [33], [36], [37].

2.2.2 Flexibility aggregators

Flexibility aggregators can be defined as entities that offer flexibility in electricity markets, encourage consumers to participate, and link suppliers and purchasers of flexibility [15]. The aggregators typically participate in the flexibility value chain as the link between prosumers and buyers. Figure 4 illustrates the buyers as grid operators in the balancing market where the aggregator compensates prosumers for their flexible resources, which, in the illustration, can be identified as PVs and batteries. Then, in trade for capacity, power, or energy, the aggregator can reserve and activate this flexibility to the grid operators for compensation. Moreover, it can be differentiated between technical and commercial aggregators, where BRPs are classified as commercial aggregators [38]. Independent aggregators (IA) and aggregators with other roles are also distinguished. To increase market competition, it is desirable to achieve an energy system with IAs [39].

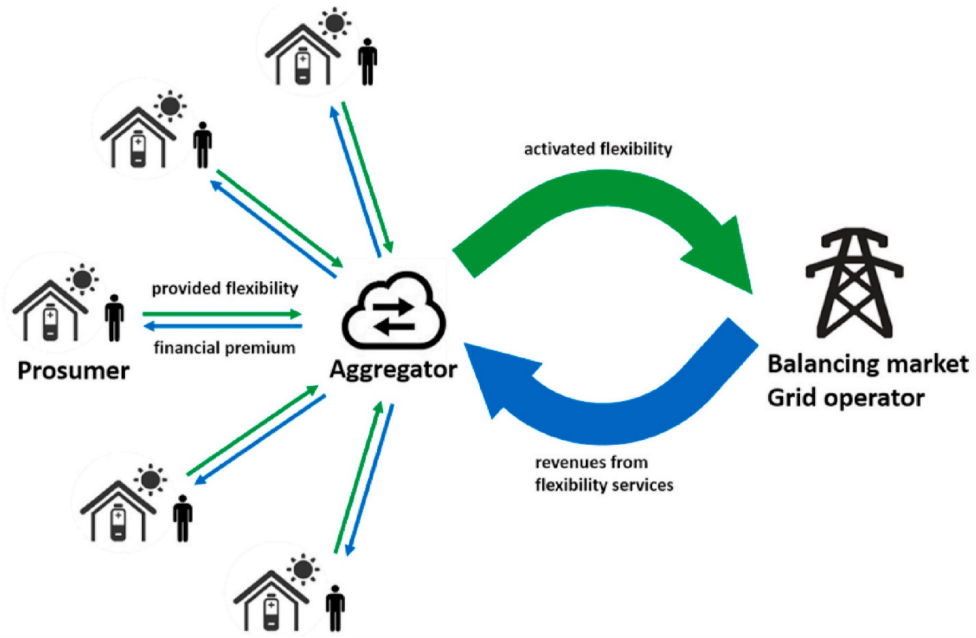

Figure 4: Flexibility value chain from an aggregator's perspective, simplified to include the buyers as grid operators, sellers as prosumers and the aggregator in between [40]

Missing aggregators is a barrier to flexibility enabling [41]. On top of this, there are several barriers for the aggregators to take significant roles to enable flexibility. These barriers include consumer trust, complexity, regulations and market structures. According to the technology company Flextools, the main barriers for both technical and independent aggregators are the following [42]:

Barriers for technical aggregators

- Difficulty in delivering standard equipment.
- Consumer scepticism to installations.
- Difficulty identifying the BRP in aggregating small loads in markets.
- Flexibility is not converted due to limitations in bids per BRP/station group in the TSO markets.

Barriers for independent aggregators

- Difficulty in accessing markets without an agreement with the BRP.
- Restrictions on which markets to access and flexibility services to deliver.
- Limited acceptance and possibility to test the role in the existing market.

Some of the identified barriers are especially relevant for EWHs. This includes regulatory and market-related barriers, ranked as the most urgent for the deployment of flexibility in the Netherlands [43]. While the lack of standards is highlighted on the regulatory side, it lacks transparency and market design for the market-based barriers. Further, policy-related issues and dealing with imbalance-costs in the market are essential. Lastly, smart meter data must be possible to access, as this data is a crucial resource for aggregators.

While there are many barriers for aggregators, there are also many technical challenges. These include baseline estimation, rebound effects and asset degradation. Another challenge is cold load pick-up, which refers to the transient surge in the load that occurs when disconnected thermal loads, such as EWHs, are reconnected. [44]. Lastly, the complexity in administration and the financial settlement, thereunder compensation to suppliers, are particularly challenging for IAs [39].

2.2.3 Balancing markets

Traditionally, flexibility has been traded in balancing markets, part of a larger structure of energy markets typically run by the TSO for energy security. Energy markets can be differentiated based on commodities like electricity and gas, where the different types of electricity markets are organised with varying time horizons, like day-ahead, future markets, intra-day, and balancing markets. In the balancing markets, balancing prices are generated based on information and bids from BRPs on surplus and deficit for generation and load.

The Nordic balancing markets are divided into time frames based on reserves. The fastest reserves are fast frequency reserves (FFR), reacting automatically within a second or two when there is low inertia in the power system. The other reserves are related to the control actions of primary, secondary, and tertiary control. These control actions are implemented sequentially, using power to recover frequency, as seen in Figure 5 [45]. When there is a drop in frequency, the primary control activates by rapidly increasing power production or reducing load. The opposite control action can also be initiated when the system frequency gets too high. Frequency containment reserves (FCR) react automatically within seconds for primary control, while secondary and tertiary control actions can be initiated to relieve the primary control and get the frequency back to its set point. For secondary control, restoration reserves (FRR) activate automatically (aFRR) or manually (mFRR) within minutes, and for tertiary control, restoration reserves react manually within tens of minutes. It is common to relate the aFRR markets to secondary control actions and the mFRR markets to tertiary control actions.

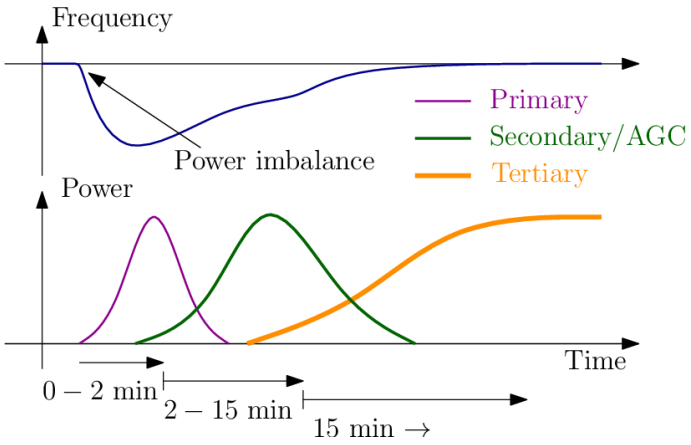

Figure 5: Frequency restoration for the TSO by primary, secondary, and tertiary control actions [45]

mFRR markets are fitting for the aggregation of EWHs because the activation of EWHs is in a feasible time frame of seconds to minutes. In the Nordics, the mFRR market provides tertiary reserves for frequency and congestion management and is further divided into a balancing market (RKM), and a capacity option market (RKOM) [46]. Both the up-regulation of increased production or reduced demand and the down-regulation of reduced production or increased demand are viable in the mFRR-market [46]. Based on the results of the eFleks-project, flexibility will be facilitated in the Nordic mFRR-markets in the coming years, primarily driven by the EU package Clean Energy for all Europeans [6]. In addition, the Nordic TSOs are currently creating a new automatic mFRR-market, changing from 1-hour to 15-minute intervals [47]. The Norwegian TSO Statnett has also claimed that the minimum bid size will be reduced from 5 and 10 MW to 1 MW in 2023 and that entry to the market should be more accessible for independent aggregators. Further, the common platform of the manually activated reserves initiative (MARI) aims to create an efficient European mFRR-market in the coming years [48].

2.2.4 Flexibility markets

Flexibility markets are emerging as an alternative class of markets for flexibility. Compared to balancing markets, the flexibility markets are especially well suited for trading flexibility on smaller scales, like regional and local levels. A flexibility market can consist of a flexibility market operator (FMO) that provides a market platform for flexibility operators (FO), also known as flexibility providers, to acquire flexibility from flexibility sources. Several types of FOs can be identified, including DSOs and BRPs. However, the trend is towards aggregators acting as the FO [39], [49]. While the FO acquires flexibility, The FMO provides a platform to which the flexibility can be traded.

NODES is an example of an existing FMO in the Nordics. The NODES flexibility market concept is shown in Figure 6 [50]. The figure shows that the TSOs can buy flexibility from reserve markets, to which microgrids can sell, while BRPs can purchase and sell to day-ahead and intra-day markets. Further, DSOs and aggregators can buy and sell flexibility through NODES directly. Aggregators must also establish flexibility contracts with prosumers that dispatch their flexibility resources. Today, the flexibility marketplace of NODES is partly functioning in Norway. While it has proven successful in some projects, it needs volume and liquidity to be fully functional [51].

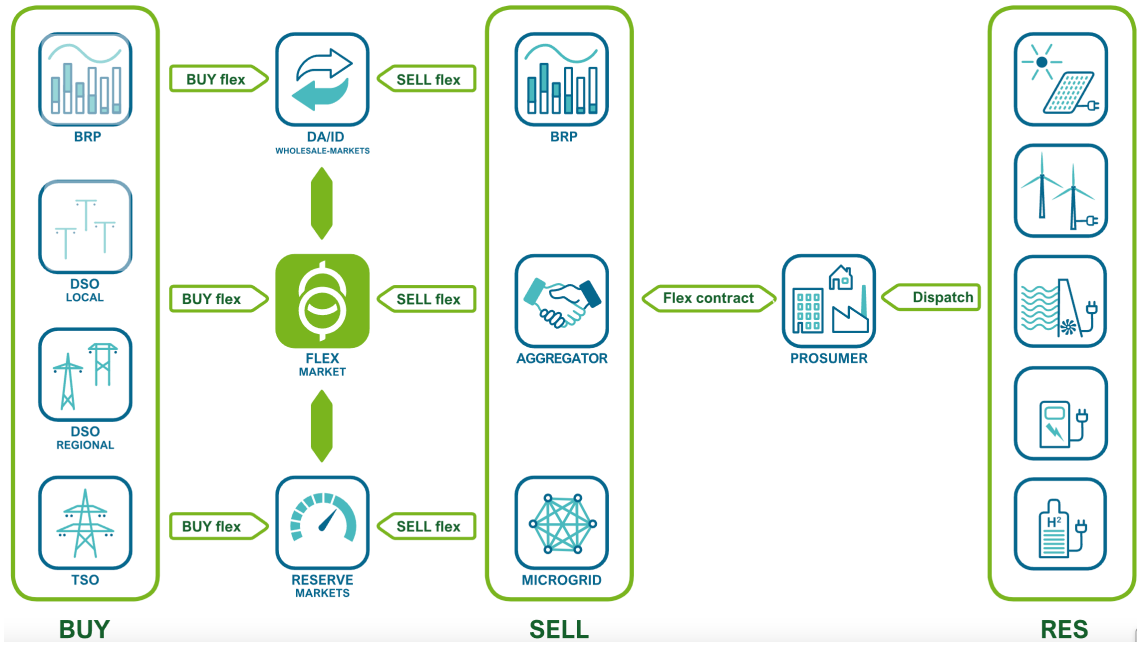

Figure 6: A model of the NODES marketplace concept for flexibility [50]

The processes of flexibility markets are not universal but can be explained in the following six steps [52].

1) Establishment of contracts between aggregators and trading partners like prosumers and DSOs.

2) Baseline estimation. For EWHs, this is expected electricity usage for the next period without flexibility. The baseline estimation is essential, as it can lead to conflicts between consumers and system operators due to opposing interests. While the consumer might want to claim a higher baseline and thus get compensated more when less energy is used at a specific time, the system operators might want to claim the opposite to compensate less.

3) Bidding to a flexibility marketplace, also called the planning phase.

4) Market clearing and validation from the market. Validation can happen through multiple iterations back and forth with the bidding. For example, the DSO might want to validate if bids violate grid constraints. However, there are many established ways of market clearing, as seen for local market clearing methods in Figure 7 [53]. This figure presents the methods by architecture, algorithm, method and solvers. The centralised optimisation methods with direct algorithms are the most common and are used in NODES. These include traditional methods like mixed-integer linear or quadratic programming (MILP and MIQP), and are ideally solved using a commercial solver [54]. Alternatively, the problem can be solved using metaheuristic methods such as genetic algorithms (GA), particle swarm optimisation (PSO) and simulated annealing (SA), as seen in Figure 7.

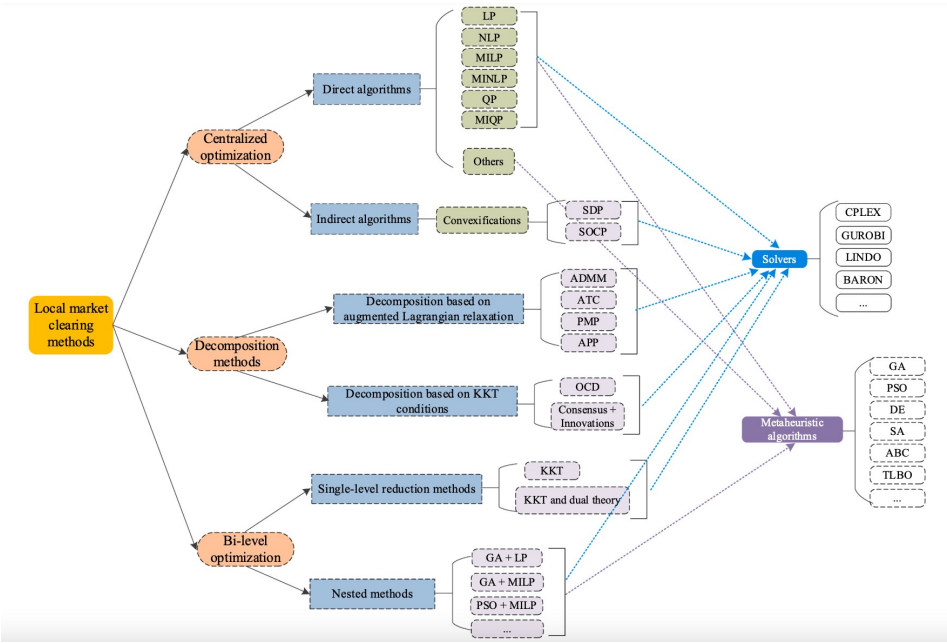

Figure 7: Local market clearing methods by architecture, algorithm, method and solvers [53]

5) Activation and operation of flexibility. This step concerns the delivery of flexibility or power over time, analogous to the intra-day market compared to the day-ahead market. Statnett has specific protocols for activation in the RK mFRR market, like the start and stop of activation within a time interval [55].

6) Settlement. A financial settlement is needed for billing. This is relevant as the buyer must be able to validate flexibility activation and aggregators must calculate and settle flexibility with the buyers, which can be BRPs, TSOs and DSOs.

2.3 Optimisation of mixed-integer problems

Optimisation can be defined as finding solutions to a problem, in most cases, the best or optimal solution, given an objective function and a list of constraints. When aiming at the best solution to a problem, optimisation can be defined mathematically as the minimisation or maximisation of some function with constraints on the decision variables [56]. Unwanted values for these variables can be modelled as constraints or penalties in the objective function. The class of optimisation problems having continuous, binary and integer decision variables or requirements is called mixed-integer problems [57]. When the variables are related linearly in the constraints, the problem can be formulated as a mixed-integer linear problem, where the objective function and all constraints are linear. Modelling problems linearly is beneficial as it is much easier to solve than non-linear problems. Problems can also be extended to mixed-integer quadratic problems using quadratic terms in the objective function. Problems with linear or quadratic objective functions and linear constraints are within the class of convex problems, which are significantly easier to solve than non-convex problems [56].

Traditionally, the optimisation methods used for mixed-integer problems have been within the class of exact methods, also known as complete methods [58], [59]. These methods can guarantee an optimal solution and be computationally efficient for mixed-integer linear problems, especially when using a commercial solver [54]. However, when problems are non-linear, approximate methods can be better suited. One class of approximate methods, rapidly growing within the domain of mixed-integer non-linear problems, are metaheuristics [58], [60]. Metaheuristics do not guarantee an optimal solution but can, in some cases, provide a good trade-off between optimality and computational efficiency [58]. However, there is still significant difficulty in scaling and applying

the methods to real-life problems.

An aggregator with flexible resources like EWHs can maximise flexibility or revenue using exact or approximate optimisation techniques. These techniques should in theory solve to an optimal or near-optimal solution accurately and computationally efficiently, so they can be run more often and scaled for many resources. In the optimisation problem of this work, the EWH temperature is continuous. At the same time, the bidding quantities in the market are integers, and the power supply of the EWHs is either on or off, making the operational status of the EWH a binary variable. Therefore, maximising flexibility from EWHs for aggregators can be formulated as a mixed-integer problem. Consequently, this section presents relevant exact and metaheuristic methods to solve the mixed-integer problem of this work.

2.3.1 Exact methods

A wide range of exact optimisation methods can be applied to solve mixed-integer problems. These include dynamic programming (DP), mixed-integer linear programming (MILP) and model predictive control (MPC). DP and MILP are mathematical optimisation methods, where MILP uses computationally efficient recursive algorithms, such as branch-and-bound or cutting planes [57]. While branch-and-bound guarantees optimality but can struggle with computational efficiency for large-scale problems, cutting plane methods can be more efficient but do not guarantee optimality. More efficient methods, like branch-and-cut, have been developed for large-scale use and are available in optimised commercial solvers like Gurobi. While DP and MILP are mathematical optimisation methods, MPC is a control strategy that solves a finite horizon open-loop optimal control problem at each instant, using the current state as the initial state for the next iteration [61]. MPC problems often use a quadratic objective function, penalising unwanted large deviations for decision variables. MPC generally provides a good trade-off between performance and robustness to uncertainty. It is, therefore, good at handling real-time operations and feedback [61], [62].

2.3.2 Metaheuristics

A metaheuristic method can be defined as an approximate high-level algorithmic framework that aims to find good solutions to complex problems [58]. Metaheuristics use probability, memory, or local search-based approaches to explore the solution space efficiently. Metaheuristic methods are generally non-deterministic, not problem-specific, and are often beneficial for non-linear problems [59].

There are many challenges with the use of metaheuristics. Firstly, it can be challenging to choose the correct method, as metaheuristics do not have a universally applicable design methodology and perform differently for different criteria, like accuracy, computational efficiency, simplicity and flexibility [58]. Secondly, there is a challenge in weighing intensification up against diversification. While intensification means prioritising good solutions, diversification means prioritising diverse solutions. Thirdly, tuning the parameters of the considered problem can be time-consuming.

Metaheuristics can be divided into local search-based methods and constructive methods [58], [59]. Common local search-based methods include simulated annealing (SA) and tabu search (TS). These methods only store one candidate solution at each time and are also known as single-state methods [60]. While SA is simple to understand and implement, TS is often better at finding good solutions quicker, given the correct tuning of parameters [60], [63].

In contrast to the single-state methods, constructive methods are population-based, meaning they evolve a population of candidate solutions. It is often applied genetic operators, such as crossover and mutation, to create new generations of solutions by the survival-of-the-fittest principle. These methods can, therefore, also be referred to as evolutionary computation. Common evolutionary methods include genetic algorithms (GA) and particle swarm optimisation (PSO) [59], [60], [63]. Evolutionary methods are generally simple and do not require high problem-specific knowledge.

On the downside, finding suitable parameters can be difficult and time-consuming, and the evolutionary methods can have difficulty scaling [64], [65]. Additionally, the search mechanisms in evolutionary methods can get stuck in locally optimal solutions, which limits the ability to find globally optimal solutions to problems. It is also difficult to debug the results using evolutionary methods. For example, it can be difficult to know if a solution from an evolutionary method is globally or locally optimal.

Of the evolutionary methods, GAs are well suited to find near-optimal solutions to problems with binary decision variables or good solutions to mixed-integer problems [66], [67]. Conversely, GAs can have inconsistent convergence to good solutions [57]. In contrast to GAs, PSO methods are better at finding good solutions to continuous problems.

A GA can consist of four steps: deciding parameters, applying a crossover function, performing mutation and selecting the best individuals for the next generation [63], [66], [67]. At first, a list of binary attributes and their starting values are decided. For simplicity, the starting values are often set at random binary values. The attributes of an individual determine the fitness value for this individual, as the attributes are included in the objective function. The objective function is, therefore, also known as the fitness function or the evaluate function. One method of including the objective function of an optimisation problem into a GA or another evolutionary method is a penalty-based approach [68]. If using a penalty-based GA, the objective function can subtract penalties for each constraint violation, thus requiring numbers for the penalisation of each constraint. Moreover, it is decided the number of generations and individuals per generation. The remaining parameters are the probabilities for crossover, mutation and bit-flip mutation [60].

After deciding the parameters, a crossover function can be initiated, creating a new generation from scratch with a size equal to that of the current generation. The crossover between two parents can be performed based on a crossover probability, where new individuals are generated based on the parents' attributes. Then, the new generation of individuals can be subject to mutations. Using a bit-flip mutation probability, mutations can occur for some individuals in the new population, swapping the binary values of some attributes for those individuals [60]. Then, the new generation, having been subject to crossover and mutation, can be compared to the old generation. If the best individual in the new generation has higher fitness than the best individual in the old generation, the new generation can be accepted or else declined. The fitness value for an individual can be determined as the value of the objective function for a maximisation problem, with the subtraction of penalties for constraint violations, if any.

Algorithm 1 gives an example of how a penalty-based GA with operations for crossover and mutation can look.

Algorithm 1 An example of a penalty-based genetic algorithm

Set the attributes and their starting values.
Decide the number of generations and individuals per generation.
Decide the probabilities for crossover ($p_{crossover}$), mutation ($p_{mutation}$) and bit-flip mutation ($p_{bit-flip}$).
Set penalties for each constraint violation.
for every generation in $number\ of\ generations$ **do**
  Divide the generation of individuals into two halves, creating pairs of parents.
  for each pair **do**
    Clone the parents' attributes into two children, one from each parent.
    Obtain the fitness value $fmax_{parents}$ to the individual with the highest fitness value in this generation.
    Generate p_1 as a random float number from 0 to 1.
    if $p_1 \leq p_{crossover}$ **then**
      Replace the attributes of the two children with the results of a two-point random crossover between the parents.
    end if
  end for
  for every child in $number\ of\ individuals$ **do**
    Generate p_2 as a random float number from 0 to 1.
    if $p_2 \leq p_{mutation}$ **then**
      for every attribute in $number\ of\ attributes$ **do**
        Generate p_3 as a random float number from 0 to 1.
        if $p_3 \leq p_{bit-flip}$ **then**
          Perform mutation by swapping the attribute to the opposite binary value.
        end if
      end for
    end if
  end for
  Obtain the fitness value $fmax_{children}$ to the individual with the highest fitness value in the new generation.
  if $fmax_{children} > fmax_{parents}$ **then**
    Replace the old generation with the new generation.
  end if
end for

2.3.3 Summary of optimisation methods

Table 3 summarises the classification, and main advantages and disadvantages of common methods for solving mixed-integer programming problems. It is provided sources of information on the advantages and disadvantages. Further, it is differentiated into the exact and metaheuristic methods, where the metaheuristic methods are differentiated into local-search-based and evolutionary algorithms.

Table 3: A summary of methods relevant for mixed-integer optimisation problems. The summary includes classification, and each method's main advantage and disadvantage

Method	**Sources**	**Classification**	**Main advantage**	**Main disadvantage**
MILP	[57]	Exact	Computational efficiency	Handle non-linearity
MPC	[61]	Exact	Handle uncertainty	Handle non-linearity
DP	[69]	Exact	Handle stochasticity	Computational efficiency
SA	[63]	Metaheuristic, local search	Simple implementation	Performance
TS	[60], [63]	Metaheuristic, local search	Computational efficiency	Ability to find optimal solutions
GA	[66], [67]	Metaheuristic, evolutionary	Handle non-linear binary problems	Handle continuous problems
PSO	[64]	Metaheuristic, evolutionary	Handle non-linear continuous problems	Handle binary problems

Generally, metaheuristics are suitable when the exact methods cannot handle the problem due to complexity or non-linearity. The choice of method for a current problem also heavily depends on the problem's characteristics. It is also possible, and often beneficial, to combine several methods, for example, local search and evolutionary metaheuristic methods. Additionally, it is essential to make the algorithms simple and flexible to be considered for real-life applications.

3 Literature Review

The literature review chapter presents the primary considerations for modelling EWHs in Section 3.1, the market participation with flexible resources in Section 3.2, and optimisation techniques relevant to problems concerning EWHs in Section 3.3. Each section is summarised with particularly applicable literature. Sections 3.1, 3.2.1 and 3.3 are based on the literature review of the specialisation project for this master's thesis with expansions of market design and optimisation methods [1].

3.1 Modelling of EWHs

This section presents an overview of how the temperature of the EWHs is modelled in relevant research and how the input data and parameters have been obtained. The single-zone and stratified models are used frequently, and while it is evident that the single-zone model is more computationally efficient, the stratified models are more accurate. On the contrary, a wide range of methods is applied to obtain the necessary input data and parameters to model the EWHs accurately.

3.1.1 Single-zone vs stratified modelling

Single-zone models are easier to set up for optimisation and more computationally efficient than stratified models [34]. This is evident by the research results, where a single-zone model incorporating some information on stratification was found 50 times more computationally efficient than the corresponding multi-layer model [34]. On the other hand, due to the higher accuracy of the temperature and power in the EWHs, many researchers apply stratified models, especially 10-layer models [33], [36], [70]. The 10-layer model has been found to be a good trade-off between accuracy and computational efficiency. It accurately captures the heating process of the water over an extended period. It is, therefore, also appropriate for integrating with electric grids over time [33], [70]. Stratified models have also notably performed better than single-zone models at predicting temperature, particularly in the higher region of the EWH [16]. The high accuracy in the temperature predictions has been applied to save electricity costs for the consumer, where a multi-layer model provided 30% cost savings with only linear constraints and 40% with non-linear constraints [34]. Although problems with non-linear constraints have achieved better results than those with linear constraints, non-linear constraints have largely been avoided due to being very computationally challenging.

3.1.2 Obtaining input data and parameters

There are several challenges within the modelling of EWHs, as the data and parametric values of hot water usage, EWH temperature and power are only rarely available. Advanced grey-box control strategies for the aggregation of EWHs have been suggested, for example, combining the differential equation of the water heater temperature from equation (3) with neural networks [71]. The model thus allows the handling of large data quantities and simultaneously captures the water heaters' physics. Still, a significant challenge is that hot water usage heavily affects the flexibility predictions [72]. Therefore, different methods to estimate hot water usage is suggested, for example using Markov chains based on the probability and mean duration of water extraction events with two-hour intervals, where both probability and duration peak at 6-8 pm [15]. While power can be estimated based on AMI data, temperature profiles can be modelled by the physical process of the EWH. For prediction of the flexibility from EWHs, strategies based on neural networks have been more common in recent years [29], [71], [73].

3.1.3 Summary of applicable literature for modelling of EWHs

Particularly relevant literature investigating the control and modelling of EWHs is presented in Table 4. The summary consists of the source of information, the primary challenge addressed, the temperature model or models used, and the main input data with its country of origin. The overview is ordered by the magnitude of the main challenges addressed: load shifting, rebound effects, uncertainty and user comfort.

Table 4: Summary of articles for EWH control- and modelling, consisting of the main challenge addressed, temperature models used, main input data and its country of origin

Ref.	**Main challenge and how it is adressed**	**Temperature model**	**Main input data**	**Input data origin**
[33]	Load shifting solved with DP	Multi-layer	Measured power	Canada
[34]	Load shifting by state estimation performing laboratory experiments	Single-zone and multi-layer	Measured power, temperature and hot water usage	Austria
[36]	Load shifting solved with MPC	Multi-layer	Electricity price	Denmark
[74]	Load shifting by state estimation performing laboratory experiments	Single-zone	Measured power	Canada
[15]	Rebound effects incorporated in a LP-optimisation constraint	Multi-layer	Measured power	Canada
[18]	Rebound effects evaluated by parameter characterisation and scenario analysis	Single-zone	Measured power	Norway
[13]	Uncertainties handled by chance-constrained optimisation	Single-zone	Hot water usage	Belgium
[16]	User temperature comfort handled by parameter estimation	Single-zone and multi-layer	Measured temperature	Canada

Both single-zone and multi-layer models are used frequently, and the input data and their country of origin are highly varying. The main challenges include grid considerations like load shifting and rebound effects, as well as other challenges like user comfort and uncertainty in modelling and optimisation.

3.2 Market participation with flexible resources

This section first presents the experienced barriers to market participation for aggregators of EWHs, emphasising the access and control of the resources. Then, experiences with market participation for aggregators in relevant research and real-life projects are presented.

3.2.1 Experienced barriers for market participation with EWHs

Many barriers to market participation by EWH aggregators have been experienced. These include having access to the resources directly or indirectly and being able to control the resources. Based on the literature, the main experienced barriers to market participation by EWH aggregators can be characterised in the following five categories [11], [13], [43].

- **Consumer considerations**. A significant challenge for the aggregators is to be allowed by consumers to control their EWHs. It is argued that EWHs cannot be controlled by aggregation but should instead be controlled individually to ensure minimal impact on user temperature comfort [75]. EWH manufacturers may not allow aggregators

to risk violating user comfort for their customers either. Combined with legionella risk, many consumers are therefore sceptical of their EWH being controlled externally by aggregators [16]. This barrier of consumer trust for aggregators is visible in the results of a Norwegian survey, where it was asked who would be most trusted for the temporary disconnection of an EWH, heating system, or EV for a shorter period [76]. The answers were 34% on BRPs, 43% on DSOs, 18% on smart house suppliers, and 15% on independent aggregators. The survey results indicate that consumers trust is an issue for aggregators.

- **Uncertainty**. The input data on hot water usage, power, and temperature of the EWHs are often uncertain, and thus, the flexibility from the EWHs is very uncertain [62], [77]. There is also often high model uncertainty when inaccurate models are used, like the single-zone models. Model uncertainty also comes from using numerical solvers and discretising time to solve the differential equation, represented in Equation (1). The discretisation of time creates significant uncertainty, especially when done over a long period [70], [78].
- **Grid considerations** like cold load pick-up and rebound effects can create significant stress on the grid [18], [44], [79]. While rebound effects have been largely avoided in the literature as it is difficult to model and not usually necessary for aggregators to implement, it has been suggested different reconnection strategies to mitigate the effects of cold load pick-up [44].
- **Regulations**. EU regulation is a decisive factor for the potential of EWH flexibility and storage in Europe. In an evaluation report commissioned by NVE, the requirements on energy efficiency in COMMISSION REGULATION (EU) No 814/2013 is particularly decisive, as these requirements can reduce the volume and flexibility of EWHs [9].
- **Market design**. ENTSO-E highlights how the market design should be changed for the future [12]. Investments in resources and integrating the resources with the markets will create higher liquidity, which is currently a big issue in flexibility markets. Additionally, the market design must better include grid constraints and consumer considerations.

3.2.2 Experience of market participation with flexible resources

Many have investigated the flexibility of EWHs and other flexible resources. Table 3.2.2 summarises particularly relevant experiences, most of them research projects. The summary includes the project, country of origin, most recent active year of the project, use of EWHs, the volume of power traded in a market, the type of market, main participants and type of grid service delivered. Some of the projects do not use EWHs but are still relevant because of the market participation and grid services.

Table 5: A summary of market participation for aggregators, with available information on the project name, country of origin, last active year, if EWHs are included, the typical trading volume of the flexible resources, market type, grid service and main participants in the project.

Ref.	**EWHs**	**Project**	**Origin**	**Year**	**Typical trading volume**	**Market and grid service**	**Participants**
[13]	Yes	-	Belgium	2021	70 kW	FCR-balancing and frequency control	TSO
[37]	Yes	-	Austria	2015	2 kW	FCR-balancing and frequency control	TSO, IA
[80]	Yes	EMPOWER	EU	2018	1 kW	Local flexibility and congestion management	DSO, IA
[81]	Yes	Smart Senja	Norway	2023	-	Local flexibility and congestion management	DSO, BRP
[51]	No	NorFlex	Norway	2022	3000 kW	Local flexibility and mFRR-balancing and congestion management	TSO, IA
[82]	No	Sthlmflex	Sweden	2023	100 kW	Local flexibility and congestion management	DSO, TSO, IA
[83]	No	iPower	Denmark	2015	-	Flexibility and congestion management	DSO, IA
[84]	No	IntraFlex	UK	2021	10 kW	Flexibility and congestion management	DSO, BRP, IA

Several projects have been completed recently or are active in many European countries. Some projects have used one or several EWHs, participating in flexibility or balancing markets to deliver frequency control or congestion management as grid services. For example, in the Smart Senja project, 30 smart EWHs were recently rolled out to contribute to congestion management by a BRP for the DSO in a NODES-based local flexibility market [81], [85]. Both TSOs and DSOs are active as flexibility buyers, while BRPs and IAs have aggregated and sold flexibility in markets. Moreover, there is a large difference in trading volumes considered, ranging from 1 kW to 3000 kW.

3.3 Optimisation problems with EWHs

Different optimisation methods, objectives, and constraints have been used for related research problems to this work. This section presents the main findings from these experiences, mainly concerning the methods, objectives and constraints, and briefly concerning uncertainty and stochasticity.

3.3.1 Methods

For optimisation problems with EWHs and other flexible resources dynamic programming (DP), mixed-integer linear programming (MILP), model predictive control (MPC) and metaheuristic methods have been applied. Contrary to MILP and MPC, variations of DP have been used to handle non-linearity but have proven computationally inefficient [33], [86]. In contrast, MILP has been efficient for scheduling problems with different DERs, like EVs, space heaters and also EWHs, but it is limited to linear problems [57] [77] [80] [87]. MPC has also been efficient for linear EWH scheduling, for example, to minimise electricity costs subject to temperature constraints and heat balance [36], [73], [78].

Some metaheuristic methods have been applied to optimise flexible resources when the problems have been too computationally expensive to solve with an exact method within a reasonable simulation time, which is often the case for problems with non-linear constraints. Although not applied directly at EWHs, local search-based metaheuristic methods have been applied in the energy domain. For example, a custom hybrid SA has been used for a grid scheduling problem involving EVs [88]. For this problem, the simulation time was reduced from 26 hours with a deterministic technique to one minute, with only a 0.1% difference in the objective value. In contrast, GAs have been applied with less success, lacking performance and computational efficiency compared to a MILP for a linear multi-layer modelled EWH problem [57].

3.3.2 Objectives

A wide range of objectives for optimisation with aggregated resources is found in the literature. These objectives include load shifting, congestion management, and frequency and voltage regulation [33]. Most studies minimise energy consumption or energy costs [89], [90]. For the studies with market participation, it is most often maximised profit, having the possibility to trade in one or several markets [87], [91], [92]. For example, EWHs have been applied to FCR markets [13]. Some also consider user temperature comfort. In one study, it is scheduled on the day-ahead and capacity market for a load aggregator of air conditioning. User comfort is handled as a linearised quadratic term in the objective function to penalise large deviations computationally efficiently [93].

3.3.3 Constraints

Different constraints are used in optimisation problems with EWHs. These include effects on the grid, like rebound effects, and user comfort temperature. Although these issues can be represented as part of the objective function, they are most commonly represented in the constraints.

Grid constraints are included in [70], where the operation of an electric boiler is constrained during the evening peak hours when there is grid congestion and under-voltages in the considered low-voltage grid. Grid effects are also successfully captured in [94], investigating DSO-aggregator interaction. A clustering algorithm to select an effective grouping of resources to deliver flexibility services to the grid solved 90% of the considered grid problems. The rebound effect is studied in detail in [18], where five flexibility activation scenarios are used, and the impact on relevant parameters is quantified. In [33], the rebound effects are reduced by clustering EWHs based on behaviour.

Some include an absolute limit for user comfort temperature as a constraint; for example, temperatures of 65 °C and 66 °C as in [77] and [78], respectively. On the contrary, [95] allows violation of user comfort with the argument that large margins can increase the demand response potential if users allow some change in comfort. Figure 8 illustrates this trade-off, where savings are achieved due to lower minimum temperature and low penalty for under-heated water [77]. Here, the decisions were mainly based on temperature and hot water withdrawal.

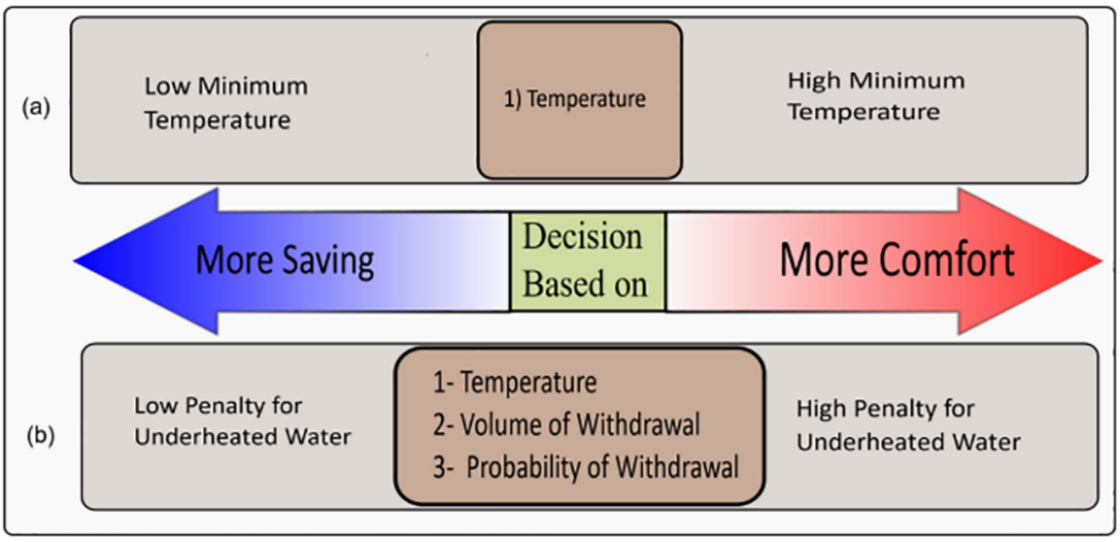

Figure 8: Trade-off between user temperature comfort and savings on electricity costs for EWHs [77]

Another technical challenge modelled in the literature is asset degradation, most commonly used for batteries [87], [96].

3.3.4 Uncertainty and stochasticity

Some relevant research includes uncertainty or stochasticity, often the uncertainty of electricity prices and the stochasticity of intermittent renewable energy generation [97]. Scenarios or probability distributions with various goals, formulations, and stochastic solution methods have represented uncertainty and stochasticity. For example, stochastic optimisation is used for EWHs in a MILP-problem [77]. Some studies also compare deterministic models with robust or stochastic models. In one study, stochastic MPC minimises energy consumption, as the deterministic approach overestimated the flexibility potential and provided greater risk to users' thermal comfort [98]. Therefore, computationally reasonable approaches to quantify demand flexibility under uncertainty are essential in future research.

3.3.5 Summary of particularly relevant literature

Table 6 summarises the main takeaways from the literature that concerns aggregator optimisation for a population of EWHs. The main takeaways are summarised based on the resources considered, the method used, the objective, the main constraints in the optimisation problem and uncertainties, if any.

Table 6: Summary of articles for optimisation of EWH for aggregators, with the representation of resources considered, choice of EWH model, the method used, objective, main constraints in the optimisation problem and uncertainties, if any.

Ref	**Resources**	**EWH model**	**Method**	**Objective**	**Main constraints**	**Main uncertainty**
[33]	73 EWHs	Multi-layer	DP	Minimise peak load	Rebound effects	Temperature
[36]	Heat pump + EWH	Multi-layer	MPC	Minimise electricity costs	Temperature	-
[86]	One EWH	Multi-layer	DP	Minimise electricity costs	Temperature	-
[57]	20 EWHs	Single-zone	MILP, GA	Minimise electricity costs	Temperature	-
[77]	One EWH	Single-zone	MILP	Minimise electricity costs and user discomfort	Temperature, power	Hot water usage

The literature is diverse on models, methods, objectives, constraints and inclusion of uncertainty. Most optimise to reduce electricity costs subject to comfort temperature constraints. Unlike most literature, [33] captures an aggregated number of EWHs with a multi-layer model. The objective here is, however, to minimise peak load, and the problem does not include any market participation. It also allows user comfort temperature violations, to the extent that the temperature is reduced to 45 °C up to 10% of the time.

To the author's knowledge, it has not successfully been optimised a group of multi-layer modelled EWHs for market participation in available research. It is, therefore, a research gap in simultaneously capturing accurate modelling, user temperature comfort and market participation for an aggregated number of EWHs.

4 Method

The chapter dedicated to the methodology is composed of five sections. The first one, Section 4.1, details the notation applied in this work. The second one, Section 4.2, then explains the modelling approach of the EWHs and the modelling-based constraints in the optimisation problem. Then, Section 4.3 presents the actions of aggregators, including reconnection strategies, and the market-based constraints used in the optimisation problem. Section 4.4 explains the optimisation method with an overview of the algorithms used to solve this work's optimisation problem. Finally, Section 4.5 presents this thesis's use cases and simulations.

4.1 Notation

This section presents the notation used for the optimisation model, presented with sets, indices, parameters and variables.

4.1.1 Sets

Hours in the planning horizon: H

Bidding periods in the planning horizon: J

Modelling periods for power and temperature in the planning horizon: T

EWHs: K

Temperature layers modelled in the EWH: L

Modelling periods for power and temperature in a bidding period: M

Modelling periods for power and temperature for the DSO to validate a bid: V

4.1.2 Indices

Time steps of hours: h

Time steps of bidding periods: j

Time steps of modelling periods for power and temperature: t

Representation of an EWH: k

Representation of a temperature layer: l

4.1.3 Problem parameters

The maximum temperature on the thermostat: T^{max}

The minimum temperature on the thermostat: T^{min}

Minimum temperature for comfort: T^{comf}

Baseline power profile: $P_{k,t}^{baseline}$ for k $\in$ K for t $\in$ T

Power of heating element per EWH : P^{he}

The number of modelling periods of power and temperature for the DSO to validate bids: DSO^{V}

Minimum bid size to deliver for the aggregator: P^{min}

Time steps of modelling periods for power and temperature in the bidding period: B

mFRR bid prices: λ_j^{mFRR} for j ∈ J

4.1.4 Variables

Continuous variables

Temperature: $x_{k,t,l}$ for k ∈ K for t ∈ T for l ∈ L

Binary variables

Bid contribution: $\delta_{k,j}^{bid}$ for k ∈ K for j ∈ J

Operational status of the EWH: $\delta_{k,t}^{power}$ for k ∈ K for t ∈ T

4.2 Modelling of EWHs

This subsection first presents the temperature models used in this work. Then, the modelling constraints used in the optimisation problem are explained. Lastly, the model uncertainty from EWH modelling is quantified.

4.2.1 Temperature models

Two different EWH temperature models are used in this work. Primarily, a multi-layer model with ten temperature layers of equal volume accurately represents the EWH to extract more flexibility and reduce consumers' risk of cold water. One heating element is placed in layer 1, second from the bottom, while the thermostat is set in layer 3, fourth from the bottom, based on the layout of the EWHs from OSO Hotwater [17]. The energy balance in the model is similar to equation (3), where the time is divided into one-minute intervals to compute the temperature and energy dynamics accurately. The energy balance equation is solved at each time instant using a fourth-order Runge-Kutta method as an initial value problem. Secondly, this work compares the multi-layer model with an equivalent single-zone model to validate the accuracy and performance of the multi-layer model. Due to a lack of real-world data, both the temperature and the power is estimated in both models.

Figures 9, 10, and 11 represent all layers' temperatures in three different EWHs before optimisation using the multi-layer model. The EWHs are denoted as EWH1, EWH2 and EWH3, with different starting temperatures and hot water usage.

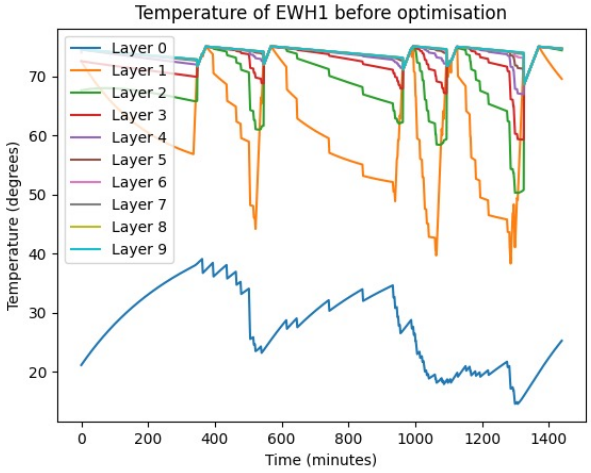

Figure 9: Temperature for all layers for EWH1 over 24 hours with a one-minute resolution multi-layer model

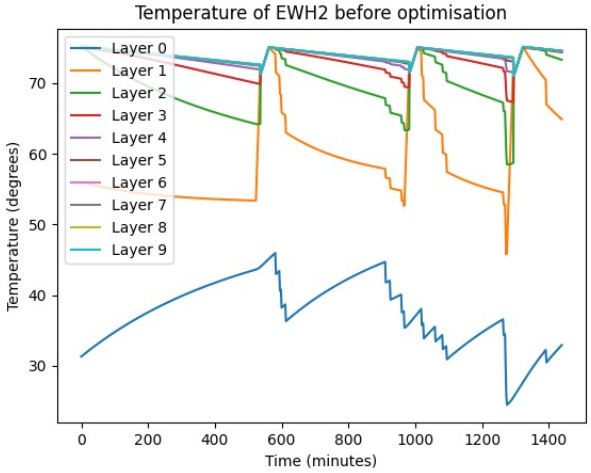

Figure 10: Temperature for all layers for EWH2 over 24 hours with a one-minute resolution multi-layer model

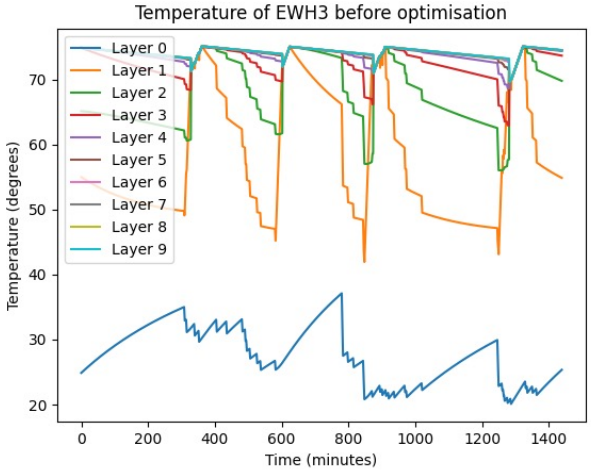

Figure 11: Temperature for all layers for EWH3 over 24 hours with a one-minute resolution multi-layer model

The temperature of EWH1 is layer-dependent, although the temperatures in the top layers are often similar due to the buoyancy effect. Layer 0 at the bottom is significantly colder than the others due to the cold water being brought in at this layer, and because the layer is below the thermostat at all times and below a thermocline most of the time. EWH1 completes five heating cycles seen by the time instants where the upper and middle layers increase rapidly in temperature. In contrast to the first EWH, the second and third EWH complete only three and four heating cycles, respectively. This is because the hot water usage associated with these EWHs is lower than EWH1.

Figures 12, 13 and 14 represent the temperatures for the same EWHs with the same hot water usage, using the single-zone model.

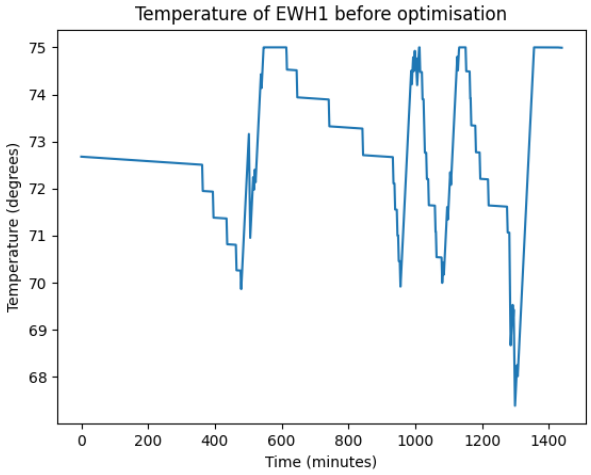

Figure 12: Temperature for all layers for EWH1 over 24 hours with a single-zone model

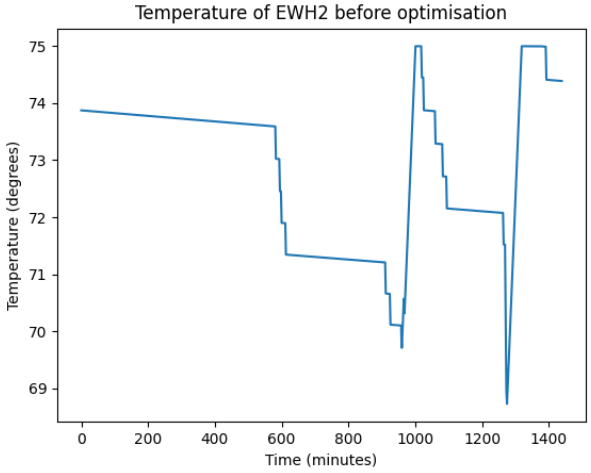

Figure 13: Temperature for all layers for EWH2 over 24 hours with a single-zone model

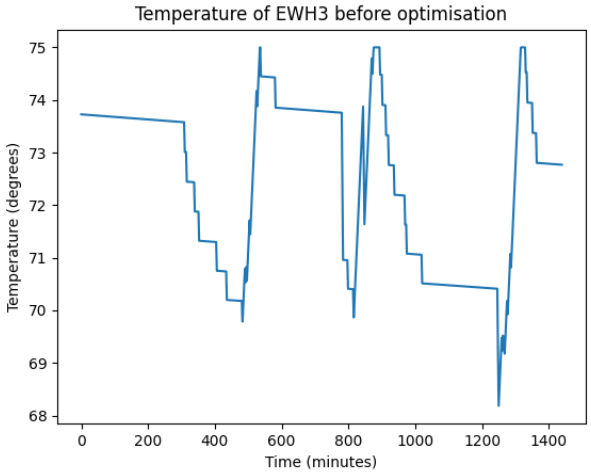

Figure 14: Temperature for all layers for EWH3 over 24 hours with a single-zone model

While EWH1, EWH2 and EWH3 completed five, three and four heating cycles with the multi-layer model, they completed only four, two and three with the single-zone model. The single-zone model underrepresents the need for heating to the extent that each EWH completes one less heating cycle per EWH over 24 hours than with the multi-layer model. The EWHs are also turned on for different lengths of time over the 24-hour horizon. While the multi-layer model resulted in the EWHs being turned on approximately 20% of the time, this number was 17% for the single-zone model, which is 15% less time than the multi-layer model. This showcases that EWHs have a higher theoretical flexibility potential for up-regulation by reduced consumption when using the multi-layer model.

4.2.2 Constraints from the EWH modelling

Equation (4) represents the temperature dynamics for each EWH as in equation (3):

$$x_{k,t,l} = x_{k,t-1,l} + f(x_{k,t-1,l \in L}) \tag{4}$$

$f(x_{k,t-1,l\in L})$ represents the temperature gradient for $k \in K$, $t \in T$ and $l \in L$. The temperature gradient is a function of the temperature in the previous time instant for all the layers, which is non-linear in three different ways:

- To model buoyancy, the layers in the 10-layer model are mixed. It is assumed that all layers must always have a temperature higher than the layer below. Suppose the heating leads to any layer having a higher temperature than the layer above. In that case, the temperature in both these two layers is set at the average temperature of the two layers. This rule-based approach makes the modelling non-linear.
- As a precautionary move to avoid increased asset degradation, an EWH must complete a heating cycle before being eligible to bid again after making a continuous flexibility contribution. Completing a heating cycle means that when an EWH is turned on, it must stay turned on until it reaches the maximum temperature or is bid. If it is bid and consequently turns on later, it must stay turned on until it reaches the maximum temperature. This rule is also non-linear in its formulation.
- To ensure that the EWHs' temperatures follow the thermostat's non-linear dynamics, the rule-based function ensures that the EWH turns off at T_{max} or when bidden. Furthermore, equation (4) also ensures that the EWH turns on at T_{min}, or as soon as a bid is completed, given that the temperature is between T_{min} and T_{comf}. The temperature of the thermostat layer is therefore constrained to the allowable temperature range of the EWH, as in equations (5) and (6):

$$x_{k,t,6} \geq T_{min} - (T_{min} - T_{comf}) * \delta_{k,j}^{bid} \tag{5}$$

$$x_{k,t,3} \leq T_{max} \tag{6}$$

  Here, the temperature is constrained for $k \in K$ and $t \in T$, based on the bids for $j \in J$.

4.2.3 Model uncertainty

There are several factors contributing to model uncertainty. The model uncertainty is reduced substantially by having short time intervals, using an efficient numerical algorithm, and with a 10-layer representation. Still, the placement of the heating element and thermostat provides significant model uncertainty.

4.3 Market participation for an aggregator with EWHs

This chapter explains the market context of this work. Firstly, it is suggested how aggregators with EWHs can operate in a market setting. Then, it is presented the market-based constraints used in the optimisation problem of this work.

4.3.1 Actions from aggregators

This work assumes that an aggregator with EWHs acts in the Nordic capacity-based mFRR-market for up-regulation. Figure 15 simplifies this process to five main actions from aggregators with EWHs.

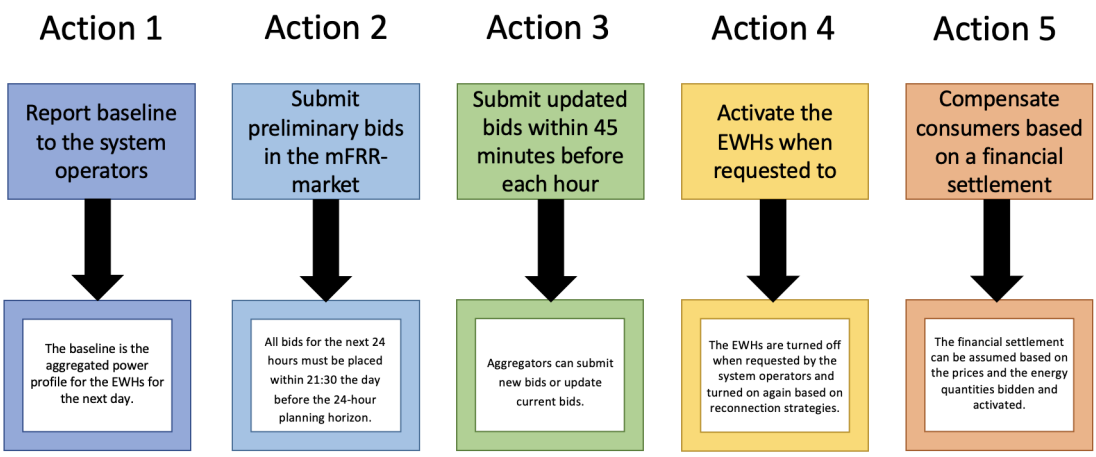

Figure 15: Block diagram for the actions of the aggregator, consisting of baseline generation, preliminary bidding, updated bidding per hour, resource activation per along the way, and compensation to consumers based on financial settlement

First, the aggregator must report a baseline of its aggregated power to the system operators before the next day starts. The system operator can be a TSO, DSO, or both. In the Nordic mFRR-market for up-regulation, the system operator is the TSO. However, as the AMI data is available for the DSOs, it can be assumed that the baseline is also reported to the DSO.

Secondly, the aggregator can submit preliminary bids for the coming 24-hour planning period in the mFRR-market before the start of the planning period. The Norwegian TSO must receive these bids within 21:30 before the next day [55]. Then, as the third action, aggregators can submit new bids or update current bids within 45 minutes of each hour in the planning horizon.

Before activating flexibility along the way, the aggregator should receive the results of the market settlement and the decision on activation volumes. Then, as the fourth action, it can be assumed that the aggregator can activate flexibility by overriding the thermostat of the EWHs. The aggregator is assumed only to turn the EWH off to deliver up-regulation in the market. It is also assumed that the aggregator decides when the EWHs are turned on when reconnection strategies are used.

This work applies three reconnection strategies to mitigate cold load pick-up and investigate its effects on the optimal solution and peak load. All three strategies are based on one EWH turning on every five minutes after providing flexibility. The reconnection for an EWH occurs after the EWH has provided flexibility and has been turned off. The strategies are different from each other by the order in which the EWHs are turned on, which are the following:

- Random selection of the EWHs.
- Selection of the EWHs with the lowest temperatures first.
- Selection of the EWHs with the lowest expected temperature 30 minutes after the flexibility provision. The expected temperature is equal to the current temperature and the expected change in temperature, assuming the EWHs are turned off, which is largely a function of hot water usage.

Before the last main action for the aggregators, the system operators should verify how much flexibility was activated. Then, action 5 for the aggregator concerns consumer compensation based on a financial settlement process. The consumer compensation should be based on comparing load with the baseline to validate how much flexibility the aggregator activated from the consumer and, thus, how much the aggregator and consumer should be compensated for.

4.3.2 Market-based constraints

It can be assumed that the flexibility from the EWHs must be above a defined minimum size directly when aggregated by the aggregator or sent to a third party. This ensures the aggregator can deliver large enough bids in the mFRR-market or large enough energy quantities to a third party acting in the mFRR-market. The minimum bid size constraint for k ∈ K and j ∈ J is presented in equation (7):

$$P^{he} * \sum_{n \in K} \delta_{n,j}^{bid} \geq P^{min} * \delta_{k,j}^{bid} \tag{7}$$

It is also assumed that an EWH can only provide flexibility if it is supposed to heat the entire bidding period in the baseline. This is represented mathematically for k ∈ K and j ∈ J in equation (8).

$$\delta_{k,j}^{bid} \leq \frac{1}{B} \sum_{t \in M} P_{k,t}^{baseline} \tag{8}$$

Further, it is assumed that it must pass a certain time so that the system operators can validate that the EWHs were turned off after being turned on initially. This is represented mathematically in equation (9).

$$\delta_{k,j}^{bid} \leq \delta_{k,j-1}^{bid} + \frac{1}{DSO^V} * \sum_{t \in V} \delta_{k,j*B-t}^{power} \tag{9}$$

Lastly, it is assumed that each EWH cannot bid and heat simultaneously in every bidding period. This is represented mathematically as in equation (10).

$$\delta_{k,j}^{power} + \delta_{k,j}^{bid} \leq 1 \tag{10}$$

4.4 Optimisation method

This section presents the optimisation method used in this work. The method consists of collecting input data, generating a baseline, and then solving and updating the optimisation problem iteratively. Figure 16 presents an overview of the method with four parts.

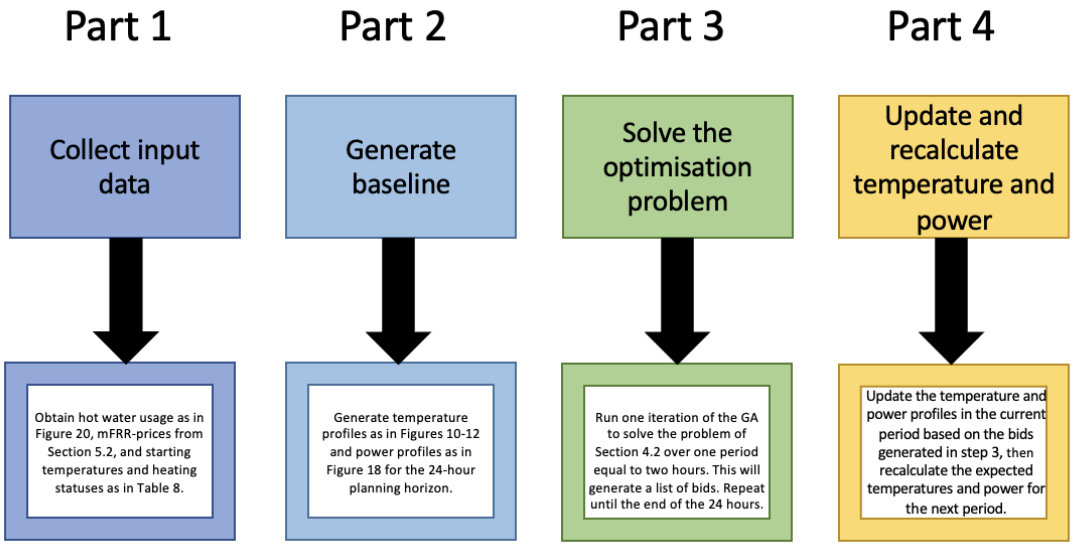

Figure 16: Block diagram of the method used in this work, consisting of the collection of input data, baseline generation, solving and updating the problem iteratively and obtaining the wanted results

Part 1 concerns this work's input data, presented in Chapter 5. Part 2 is the baseline generation, presented as a distinct subsection. Then, parts 3 and 4 concern how the optimisation problem is solved iteratively. This work's optimisation problem is presented in two subsections; one for the mathematical formulation of the optimisation problem and one for the algorithms used to solve it.

4.4.1 Baseline generation

Based on the input data, a power and temperature baseline is created following the temperature dynamics from equation (4), within the boundaries of inequalities (5) and (6). This means that when an EWH reaches T_{min}, the EWH turns on in the current time step and stays on until T_{max} is reached, and then turns off and stays off until T_{min} is reached again. It is assumed that the baseline is reported to the DSO after completion. In Figure 17, the aggregated baseline power profile with 100 EWHs for one 24-hour simulation using the multi-layer model is shown.

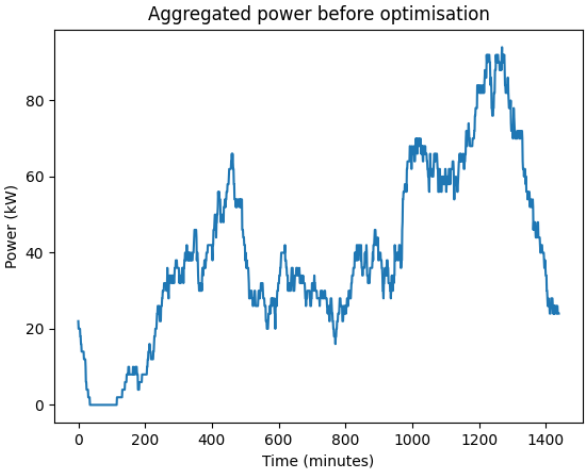

Figure 17: Aggregated baseline power profile for 100 EWHs over 24 hours using the multi-layer model

In this simulation, slightly more than 10% of the EWHs are turned on at the start, as the aggregated power is above 20 kW. Then, there is a distinct peak in the morning and even higher peaks in the afternoon and evening, almost reaching 100 kW, equivalent to slightly less than half of the EWHs being turned on simultaneously.

4.4.2 Mathematical formulation of the optimisation problem

The mathematical formulation of the optimisation problem consists of an objective function and the constraints deduced in previous chapters. The primary objective of the work is to maximise flexibility from the EWHs, which can be represented as $max\ z = \sum_{k \in K} \sum_{j \in J} \delta_{k,j}^{bid}$, where individual bid contributions are maximised. A complete mathematical formulation of the problem can be written as the following:

$max\ z = \sum_{k \in K} \sum_{j \in J} \delta_{k,j}^{bid}$

subject to

(1) $x_{k,t,l} = x_{k,t-1,l} + f(x_{k,t-1,l \in L})$ for k ∈ K for t ∈ T for l ∈ L

(2) $x_{k,t,3} \geq T_{min} - (T_{min} - T_{comf}) * \delta_{k,j}^{bid}$ for k ∈ K for t ∈ T

(3) $x_{k,t,3} \leq T_{max}$ for k ∈ K for t ∈ T

(4) $P^{he} * \sum_{n \in K} \delta_{n,j}^{bid} \geq P^{min} * \delta_{k,j}^{bid}$ for k ∈ K for j ∈ J

(5) $\delta_{k,j}^{bid} \leq \frac{1}{B} \sum_{t \in M} P_{k,t}^{baseline}$ for k ∈ K for j ∈ J

(6) $\delta_{k,j}^{bid} \leq \delta_{k,j-1}^{bid} + \frac{1}{DSO^V} * \sum_{t \in V} \delta_{k,j*B-t}^{power}$ for k ∈ K for j ∈ J

(7) $\delta_{k,j}^{power} + \delta_{k,j}^{bid} \leq 1$ for k ∈ K for j ∈ J

4.4.3 Solving the optimisation problem iteratively with a GA and a reference algorithm

Based on the baseline of power and temperature, the optimisation problem is solved with a GA and a simplified reference algorithm. The reason the optimisation problem cannot be solved by an exact method as formulated in section 4.4.2 is that constraint (1) from equation (4) is non-linear. Adapting the non-linear constraint to a linear constraint would imply non-optimality and infeasible solutions. Therefore, metaheuristic algorithms like the GA are better suited than exact methods for this problem, as the metaheuristic methods can handle non-linear constraints. Of the metaheuristic algorithms, the GA fits this problem as it is well suited to handle binary variables, which is the case for the bid contributions and operational status of the EWHs. Therefore, a GA is primarily used in this work. More specifically, this work uses a penalty-based GA, meaning the objective function from Section 4.4.2 also subtracts penalties for each constraint violation in each solution run through the objective function. The penalties ensure that most or all optimal solutions are feasible, depending on how significant the penalties are. In addition to the GA, a simple reference algorithm was developed to compare and validate the performance of the GA.

When using the GA for a problem like this, bids can be optimised based on prices, minimum bid size constraints and other criteria. However, the problem of this work is too computationally intensive if solved over the entire planning horizon. Additionally, the algorithm should be updated regularly, as it is unknown if the flexibility will activate along the way, and the power and temperature profiles are subject to significant uncertainty. Therefore, the problem of this is solved iteratively through the planning horizon. Algorithm 2 shows how the problem is solved.

Algorithm 2 Solving the optimisation problem iteratively with a genetic algorithm

Generate a baseline of power and temperature over the 24-hour planning horizon.
for every optimisation period **do**
  Solve the problem of Section 4.4.2 with a GA, for example as presented in Algorithm 1, generating flexibility in the form of bid contributions per EWH.
  Remove infeasible bid contributions, if any.
  Based on the resulting bids, update the power and temperature profiles for the next bidding period.
end for

After the baseline, the iterative GA includes three steps:

- Solve the optimisation problem as presented in Section 4.4.2 for a certain optimisation period. The length of the optimisation period is low enough to be computationally manageable and long enough to optimise bids based on certain criteria, which in this case, is the minimum bid size constraint. This work uses an optimisation period of two hours, providing a good trade-off.
- For each period, check if the optimal bids are feasible, meaning they do not violate any constraints, and remove the constraint-violating bids, if any. This check is done as the penalty-based GA does not guarantee feasible solutions if the penalty is too low. Additionally, it allows checking if the bids are initiated along the way, so the power and temperature schedules can be updated accordingly.
- Simulate the updated prediction for power and temperature schedules for the coming period, assuming no bids. Then, the power and temperature are used as input for the next iteration of the GA.

While the GA applies optimisation to find the most flexibility subject to the constraints, the reference algorithm is based on simple rules. This significantly reduces the algorithm's simulation time compared to metaheuristic or exact methods. Algorithm 3 shows how the reference algorithm is applied.

Algorithm 3 Solving the optimisation problem iteratively with a reference algorithm

Generate a baseline of power and temperature over the 24-hour planning horizon.
for every bidding period **do**
  for every EWH **do**
    Set preliminary bid contribution if constraints (1)-(3) and (5)-(7) are satisfied.
  end for
  Remove all bid contributions if constraint (4) is violated.
  Based on the resulting bids, update the power and temperature profiles for the next bidding period.
end for

As in the GA, the power and temperature in the reference algorithm are first imported from the baseline. Then, for each bidding period in the 24-hour planning horizon, a bid contribution is preliminarily added for every EWH that does not violate any of the constraints (1)-(3) or (5)-(7) if bidden. Then, if the number of bids satisfies constraint (4) concerning the minimum bid size constraint, all the bids are kept, else they are discarded for that bidding period. After this constraint check, the power and temperature are updated based on the bids, and the algorithm goes to the next bidding period.

The advantage of the reference algorithm is its simplicity and computational efficiency. The main disadvantages are that the method does optimise bids for prices and coordinates bids based on the minimum bid sizes. It does, therefore, not dispatch flexibility optimally over time.

4.5 Use cases and simulations

This section presents the use cases and simulations conducted in this work. Each use case has a distinct temperature model, optimisation method, and number of EWHs run a certain number of times on different hardware with different starting values. However, the simulations also have several aspects in common. For all simulations, the minimum bid size, P_{min}, corresponds to 10% of the EWHs being turned on. This power quantity equals 2 kW for the simulations with 10 EWHs, 6 kW for the simulations with 30 EWHs and 20 kW for the simulations with 100 EWHs. While many combinations of the mentioned considerations exist, this work has selected 24 combinations. Figure 18 summarises the step-wise process of choosing these use cases. The main steps of simulations, marked in blue, have a multi-layer temperature model and use the GA as the optimisation method. In parallel, two steps are marked red to verify the multi-layer GA to a single-zone model and a reference algorithm as the optimisation method.

For simplicity, the numbers of generations and individuals per generation for every optimisation period in every simulation using the GA are equal to a fixed integer multiplied by the number of feasible bids for that period, denoted as *scaling factor*. The number of feasible bids over the optimisation period is the sum of feasible bids in each bidding period, which for every bidding period is equal to the sum of EWHs being turned on in the baseline in the entirety of that bidding period. For example, with a portfolio of 10 EWHs in the period 04:00-06:00, if one of them is turned on between 04:03 and 04:32 and one from 04:29 to 05:03, then the number of feasible bids for that bidding period is three, consisting of the first EWH in the bidding period 04:15-04:30, and the second EWH in the periods 04:30-04:45 and 04:45-05:00. With this example, the simulations using a scaling factor of one would run for three generations with three individuals per generation. However, if the simulations used a scaling factor of two, it would run for six generations with six individuals per generation and similarly for nine with a scaling factor of three. In comparison to running a fixed number of generations and individuals per generation, this solution will run for more generations, with more individuals per generation in the periods where there are many available bids, and therefore crucial to maximising the flexibility, and for a lower number of generations, with fewer individuals per generation when there is little or no flexibility to find, reducing the simulation time substantially. For simplicity, this work uses scaling factors equal to one, two or three to illustrate the differences in flexibility and simulation time when doubling and tripling the number of generations and individuals per generation in the GA.

All simulations were conducted by use of Python 3.10. The Deap library was used for the simulations with the GA, while the reference algorithm did not use any external libraries. All simulations were run on servers from the Idun cluster by NTNU High Performance Computing Group with one compute node with an eight mpi process and 10 GB memory.

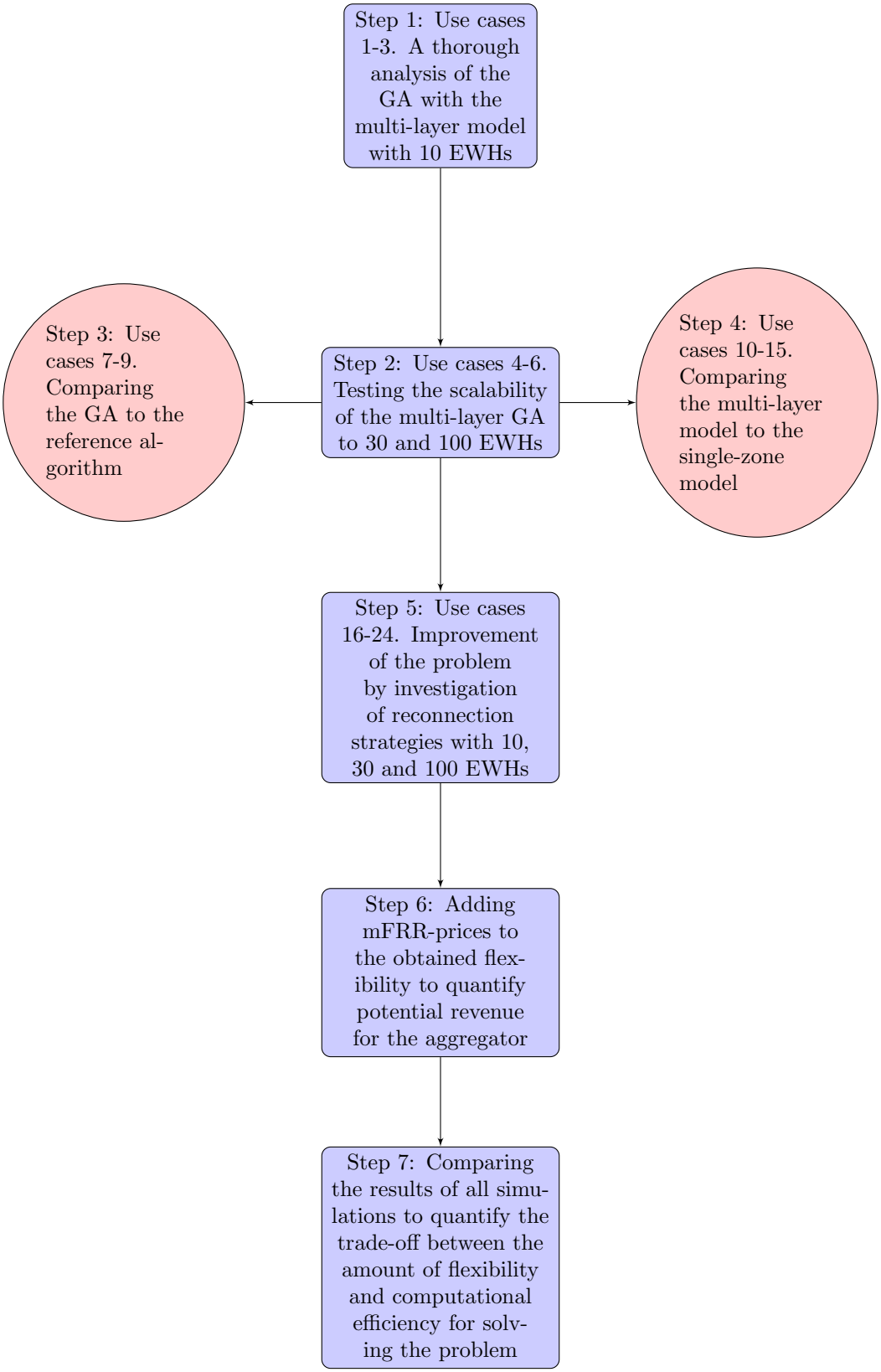

Figure 18: Flow chart of the optimisation algorithm, consisting of the main activities with the multi-layer GA in blue and the verifications to the multi-layer GA in red.

4.5.1 Step 1: Use cases 1-3 for 10 EWHs with a multi-layer temperature model and GA as optimisation method

This work first thoroughly analyses the performance with the GA using ten multi-layer modelled EWHs. In use cases 1-3, ten simulations are conducted for ten sets of random starting temperatures and power, 100 for each use case. This is primarily to quantify the main results for the problem with a large sample size to account for the randomness of the GA and the starting values for power and temperature. In most other use cases, the number of simulations is reduced to ten for computational reasons. For direct comparison between the scaling factors, use cases 1-3 are only differentiated by having a scaling factor of 1, 2 and 3, respectively.

4.5.2 Step 2: Use cases 4-6 for 30 and 100 EWHs with a multi-layer temperature model and GA as optimisation method

Use cases 4-6 primarily investigate the trade-off between flexibility and simulation time for the GA when increasing the number of multi-layer modelled EWHs. 30 EWHs are applied in use cases 4 and 5, where ten simulations are conducted with one simulation per ten sets of starting values for power and temperature. To investigate the trade-off between optimality and computational efficiency with 30 EWHs, use cases 4 and 5 have scaling factors of 1 and 2, respectively. Then, use case 6 similarly has ten simulations but with 100 EWHs and a scaling factor of 1. Scaling factors 1 and 2 are used for 30 EWHs and only 1 for 100 EWHs because it is very computationally expensive to conduct simulations simultaneously with many EWHs and a high scaling factor.

4.5.3 Step 3: Use cases 7-9 for 10, 30 and 100 EWHs with a multi-layer temperature model and a reference algorithm as optimisation method

To validate the performance and simulation times of the GA, use cases 7-9 solves the same problem as in use cases 2, 5 and 6 with the reference algorithm rather than the GA. The problem is solved for 10, 30 and 100 EWHs to assess the performance of the GA compared to the reference algorithm for different numbers of EWHs in the portfolio. As the reference algorithm cannot produce different results for a set of starting values for power and temperature, ten simulations were conducted for each use case, each with a unique set of starting values for power and temperature.

4.5.4 Step 4: Use cases 10-15 for 10, 30 and 100 EWHs with a single-zone temperature model for both optimisation methods

To validate the multi-layer temperature model, use cases 10-15 have the single-zone temperature model using the GA and reference algorithm alternately, with 10, 30 and 100 EWHs. The simulations with the GA have scaling factors of 2, 2 and 1, which directly compare to use cases 2, 5 and 6, respectively. These use cases are chosen because their scaling factors lead to good trade-offs between flexibility and simulation time for 10, 30 and 100 EWHs. To compare with an equal number of simulations as in the compared use cases, 100 simulations in use case 10 are conducted for a direct comparison with use case 2. Likewise, ten simulations are conducted in use cases 11-15, each with unique starting values for power and temperature.

4.5.5 Step 5: Use cases 16-24 for 10, 30 and 100 EWHs with a multi-layer temperature model, GA as optimisation method and reconnection strategies

Three reconnection strategies are applied for 10, 30 and 100 multi-layer modelled EWHs using the GA in the last nine use cases. For every use case, ten simulations are performed with unique starting values for power and temperature. Similarly to use cases 10-15, these use cases have scaling of 2, 2 and 1 for 10, 30 and 100 EWHs, respectively.

4.5.6 Summary of steps 1-5

Table 7 summarises the 24 use cases with temperature model and reconnection strategy, if any, optimisation method, number of EWHs, scaling factor for the simulations using the GA and the number of simulations conducted per use case.

Table 7: Use cases in this work, presented with temperature model and reconnection strategy, optimisation method, number of EWHs, scaling factor in the GA and number of simulations conducted

Use case	**Temperature model**	**Optimisation method**	**Number of EWHs**	**Scaling factor in the GA**	**Number of simulations**
1	Multi-layer	GA	10	1	100
2	Multi-layer	GA	10	2	100
3	Multi-layer	GA	10	3	100
4	Multi-layer	GA	30	1	10
5	Multi-layer	GA	30	2	10
6	Multi-layer	GA	100	1	10
7	Multi-layer	Reference algorithm	10	-	10
8	Multi-layer	Reference algorithm	30	-	10
9	Multi-layer	Reference algorithm	100	-	10
10	Single-zone	GA	10	2	100
11	Single-zone	Reference algorithm	10	-	10
12	Single-zone	GA	30	2	10
13	Single-zone	Reference algorithm	30	-	10
14	Single-zone	GA	100	1	10
15	Single-zone	Reference algorithm	100	-	10
16	Multi-layer + reconnection strategy 1	GA	10	2	10
17	Multi-layer + reconnection strategy 2	GA	10	2	10
18	Multi-layer + reconnection strategy 3	GA	10	2	10
19	Multi-layer + reconnection strategy 1	GA	30	2	10
20	Multi-layer + reconnection strategy 2	GA	30	2	10
21	Multi-layer + reconnection strategy 3	GA	30	2	10
22	Multi-layer + reconnection strategy 1	GA	100	1	10
23	Multi-layer + reconnection strategy 2	GA	100	1	10
24	Multi-layer + reconnection strategy 3	GA	100	1	10

4.5.7 Step 6: Applying mFRR-prices

Based on the results of these use cases, step 6 applies mFRR-prices to quantify the potential revenue for the aggregator based on the obtained flexibility. The mFRR-prices are important as aggregators can be assumed to want to maximise revenue from flexibility rather than the flexibility itself. Therefore, the objective function of the problem can be extended to $max\ z = \sum_{k \in K} \sum_{j \in J} \delta_{k,j}^{bid} \lambda_j^{mFRR}$, where λ_j^{mFRR} is the mFRR market price for a considered bidding period j. The power provided by an EWH in a time instant is multiplied by the length of the time instant to obtain the energy quantity, multiplied by the prices in monetary value per energy quantity, resulting in a monetary value. In this work, the time is one hour, and the currency is EUR.

4.5.8 Step 7: Quantifying the results

The main results of the work are the flexible energy and revenue, as well as the algorithm's simulation time and change in peak load compared to the baseline. Therefore, the results of all simulations are compared in step 7 to quantify the trade-off between the amount of flexibility and computational efficiency for solving the problem. The flexibility is presented in kWh per EWH per day, while the revenue is found by multiplying this with 1/1000 of the mFRR-price given in EUR/MWh, resulting in the revenue in EUR. The algorithm's simulation time is rounded off to the nearest minute, while the change in peak load compared to the baseline is the percentage change of the highest minutely peak over the planning horizon. When running several simulations per use case, the average results, best results and standard deviations from the samples are also found.

5 Case Study

This chapter presents the case study in this master thesis concerning EWH modelling, market participation with EWHs, and optimisation of EWHs. The chapter is divided into three sections, each presenting input data. The first section presents the input data for modelling EWHs, particularly the hot water usage and chosen parameters for starting power and temperature values. The second section is dedicated to market participation, presenting three price scenarios used in this work. Finally, the third section concerns the optimisation problem, showing the chosen dimensions of sets and the parameters used in the GA.

5.1 Input data for the EWHs

Besides the hot water usage, the physical parameters of the EWHs are equal to those in Table 1. In addition, the conductivity coefficient for each layer in the model has a dimensionless value of 2.21, equal to that used for a 10-layer model in relevant literature [33]. The temperature setpoints of the thermostat are set at typical values for Norwegian operation; 70 °C and 75 °C, respectively [24]. To represent user comfort, a temperature of 65 °C is used, as in relevant literature [77]. This temperature is considered in layer 5, the sixth layer starting from the bottom, located in the middle of the tank.

5.1.1 Hot water usage

To represent Nordic behaviour, the hot water usage is synthetically generated from a stochastic load model from Sweden, last updated in 2018 [99], [100], [101]. The model is based on hot water withdrawals for bathing, showering and miscellaneous activities. As standard parameters, 16 L per minute is used for six minutes to represent bathing, 10 L per minute for four minutes to represent showering and 4 L per minute for two minutes to represent miscellaneous activities. The miscellaneous activities occur with a 1% likelihood per minute and represent the many minor withdrawals from food preparation, hand washing, dishwashers and washing machines. Unlike other activities, bathing and showering are based on time-of-use data [29].

This work uses data for 100 EWHs for up to five days. The data is mainly based on the standard parameters of the stochastic load model, with some minor changes, including using 14 L instead of 16 L for bathing. For approximately 92% of the minutes, no hot water is extracted. Of the minutes with withdrawals, 94% of the occurrences are at 4 L, while only 5% of the withdrawals are 10 L, and 1% 14 L. The average minutely withdrawals for 24 hours are shown in Figure 19. For comparison purposes, as most of the literature presents the hot water usage hourly, Figure 20 presents the average hourly withdrawals for 24 hours. Lastly, all elements in the hot water usage are scaled such that the share of time the EWHs are turned on is around 20%, which represents a realistic operation of the EWHs [13].

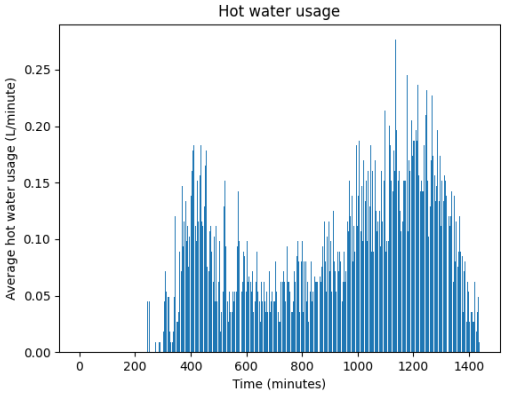

Figure 19: Average hot water usage [L] per minute over 24 hours from the aggregated profile of 100 EWHs from Sweden [99], [100], [101]

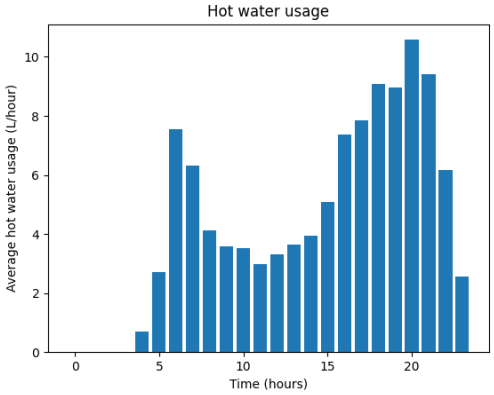

Figure 20: Average hot water usage [L] per hour over 24 hours from the aggregated profile of 100 EWHs from Sweden [99], [100], [101]

The hot water extraction has a distinct peak in the morning and an even higher and long-lasting peak in the afternoon. The profile of hot water usage matches well compared to relevant literature [15], [33].

5.1.2 Starting values of power and temperature

To investigate likely starting values of $x_{k,0,l}$ and $\delta_{k,0}^{power}$, the start temperatures were first set at $x_{k,0,l} = (T_{max} + T_{min})/2$, while $\delta_{k,0}^{power}$ for each EWH had a 10% chance of being equal to 1, e.g. the EWH being turned on at the start. Then, ten simulations of the baseline for five days each were conducted to find the typical values of $x_{k,t,l}$ and $\delta_{k,0}^{power}$ at 00:00 after five days. The average values for temperature in each layer and the standard deviation in each layer were registered to obtain a distribution of the temperatures.

The end values for power and temperature were interpreted as the starting values for power and temperature at the beginning of the planning horizon. The average share of EWHs turned on at 00:00 after five days was 9.2% for the multi-zone model and 10.6% for the single-zone model. Based on these results, the EWHs were given a 10% chance of being turned on at the start of the planning horizon. For simplicity, the starting temperature in each layer for each EWH was set as a random sample from a standard Gaussian distribution with an expected value of the average temperature with a standard deviation equal to the average found for that considered layer. Table 8 displays the average temperatures at 00:00 for each of the ten layers between the 100 EWHs after running a five-day simulation with the multi-layer model. The standard deviations for these values are also included. For the corresponding single-zone model, the average temperature was 73.4 °C with a standard deviation of 1.4 °C.

Table 8: Average temperatures and standard deviation of the 100 EWHs after five days of simulation using the multi-layer temperature model

Layer	**1**	**2**	**3**	**4**	**5**	**6-10**
Average temperature (°C)	24.2	59.6	69.9	73.3	74.2	74.4
Standard deviation (°C)	5.3	9.3	4.5	1.6	0.7	0.5

5.2 Price scenarios in the mFRR-market

In addition to the minimum bid size, the parameters related to the market are the mFRR-prices. Although not part of the optimisation algorithm, this work applies three different price scenarios after the optimisation process. For simplicity, these were all chosen among the available data for hourly mFRR-prices for the price area NO1 from January 2023 [102].

- Scenario 1: Average prices. The average mFRR-price for January 2023 in NO1 was 128.34 EUR/MWh. To represent this price through a typical day, it is used the prices of January 10th 2023, which had an average price of 128.84 EUR/MWh. This day had a minimum price of 55.77 EUR/MWh and a maximum of 170.00 EUR/MWh.
- Scenario 2: Volatile prices. To represent a day with volatile prices, it is used the prices of January 19th 2023 with an average price of 187.56 EUR/MWh, a minimum of 102.31 EUR/MWh and a maximum of 700.00 EUR/MWh.
- Scenario 3: High prices. The highest average price in January 2023 occurred on January 23rd 2023 at 243.33 EUR/MWh, with a minimum of 134.10 EUR/MWh and a maximum of 700.00 EUR/MWh.

5.3 Optimisation parameters

This section presents the dimensions of sets in the optimisation problem and the parameters used in the GA.

5.3.1 Dimensions of sets

Because the hot water usage is given in hourly values over one day, it is used a 24-hour planning horizon. Consequently, the number of bidding periods is 96, assuming four bidding periods each hour. The number of modelling periods for power and temperature is assumed to equal the number of minutes in the planning horizon, which is 1440. This equals 15 modelling periods of power and temperature per bidding period. The number of layers is ten, and the number of minutes for bid validation is five. The dimensions of sets used in this case study are, therefore, the following:

Hours in the planning horizon: $H = 24$

Bidding periods in the planning horizon: $J = 96$

Modelling periods for power and temperature in the planning horizon: $T = 1440$

Temperature layers modelled in the EWH: $L = 10$

Modelling periods for power and temperature in a bidding period: $M = 15$

Modelling periods for power and temperature for the DSO to validate a bid: $V = 5$

5.3.2 Parameters used in the GA

This work applies a penalty-based GA as it is presented in Algorithm 1. In addition to the attributes, the GA uses five parameters: the number of generations and individuals per generation and the probabilities for crossover, mutation and bit-flip mutation. Penalties are also applied in the objective function and random starting values for the attributes. The attributes in this problem are, for each EWH in each bidding period in an optimisation period, whether the EWH is bidden in that bidding period. If an EWH is bidden in a bidding period, then the attribute's value is equal to 1, and 0 otherwise. The number of attributes per individual equals the number of EWHs multiplied by the number of bidding periods in the optimisation period, which is eight 15-minute periods over

two hours. This summation makes the number of attributes equal to 80 for the simulations with 10 EWHs in the portfolio, 240 with 30 EWHs in the portfolio and 800 with 100 EWHs in the portfolio. The starting values for the attributes are, for simplicity, all set random binary values of one or zero.

As presented in Chapter 4.5, the number of generations and individuals per generation is chosen based on the number of feasible bids for each optimisation period. While these values vary for each period, the other parameters remain constant for each simulation. Of the constant parameters, this work uses a mutation rate of 0.2 and a crossover rate of 0.8, as commonly found in the literature [103], [104]. Although the bit-flip mutation probability is typically recommended at the inverse of the number of attributes, which would be 1/80, 1/240 and 1/800 with 10, 30 and 100 EWHs in the portfolio, this work uses a bit-flip mutation probability of 1/20 to ensure more mutations of attributes [105]. This ensures diversification is prioritised sufficiently against intensification in the search for good solutions.

For simplicity, the penalties for each constraint violation are set at one, aiming to be high enough to ensure most constraint-violating bids are removed and low enough to not lose out on promising solutions that barely violate one or more constraints along the way. Then, when each optimisation period ends, if any of the bids in the final solution from that optimisation period violate any constraint, these bids are removed from the solution.

6 Results

This chapter includes the most important results from the simulations of the 24 use cases used in this work. Section 6.1 presents the results from the multi-layer GA. Section 6.2 then compares these results to the reference algorithm and Section 6.3 to the single-zone model, using both algorithms. Further, the results of the multi-layer GA with three different reconnection strategies are presented in Section 6.4. Lastly, mFRR-prices are added in Section 6.5, and the results are summarised in Section 6.6.

6.1 Results with the multi-layer genetic algorithm

6.1.1 Use cases 1, 2 and 3 - 10 EWHs

Use cases 1, 2 and 3 with 10 EWHs, a GA and a multi-layer model were all run for 100 simulations with ten sets of identical starting values and 10 EWHs per simulation. Table 9 presents the results from these use cases as the average, highest average and highest recorded flexible energy of the 100 simulations, average simulation time and average change in peak load compared to the baseline. Here, the highest average means the average of the ten highest recordings, one per each set of identical starting values. Then, Figure 21 shows the distribution of achieved flexible energy among the 100 simulations, where each of these use cases had a standard deviation of 0.4 kWh/EWH.

Table 9: Results from use cases 1, 2 and 3 with the multi-layer GA - 10 EWHs

Use case	**Scaling**	**Average flexible energy [kWh/ EWH]**	**Highest average flexible energy [kWh/ EWH]**	**Highest flexible energy [kWh/ EWH]**	**Average simulation time [min]**	**Average change in peak load**
1	1	3.8	4.4	4.8	5	8%
2	2	4.3	5.0	5.4	20	4%
3	3	4.4	5.0	5.3	42	5%

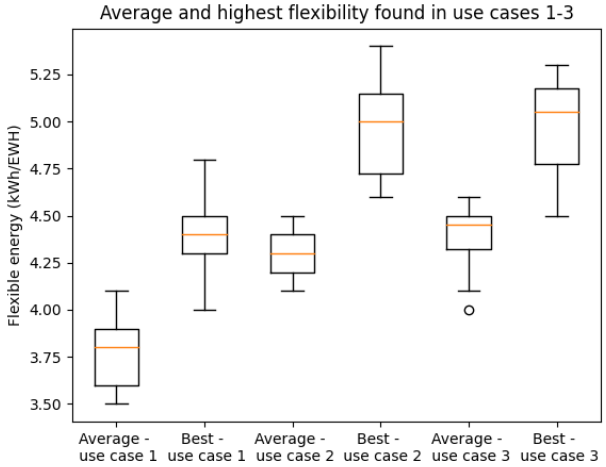

Figure 21: Results from use cases 1, 2 and 3 showing the distribution of average and best values for flexible energy per EWH. The results are presented as box plots with a box from the first to the third quartile, a vertical line representing the median, and outliers represented as dots.

The flexibility in use case 2 was, on average, 13% higher than in use case 1 and 14% for the best simulation. However, use case 2 had a simulation time four times as high as use case 1. Moreover, the increase in peak load was 4% less compared to use case 1. On average, the flexibility in use case 3 was 16% greater than in use case 1 and 14% higher for the best simulation. However, it took ten times as long to run. The increase in peak load was 3% lower in use case 3 than in use case 1. Compared to use case 2, the level of flexibility provided by use case 3 was similar, but the simulation time and peak load were significantly higher.

6.1.2 Use cases 4 and 5 - 30 EWHs

Use cases 4 and 5 with a GA and a multi-layer model were all run for ten simulations and 30 EWHs. Table 10 presents the results from these use cases as the average, highest and standard deviation of the recorded flexible energy between the ten simulations, average simulation time and average change in peak load compared to the baseline.

Table 10: Results from use cases 4 and 5 with the multi-layer GA - 30 EWHs

Use case	**Scaling**	**Average flexible energy [kWh/ EWH]**	**Highest flexible energy [kWh/ EWH]**	**Standard deviation [kWh/ EWH]**	**Average simulation time [min]**	**Average change in peak load**
4	1	2.9	3.3	0.3	73	4%
5	2	3.3	3.8	0.2	187	7%

On average, the flexibility in use case 5 was 14% higher than in use case 4 and 15% higher for the best simulation, although the simulation time was 2.5 times longer. However, the increase in peak load was 3% higher compared to use case 4.

Compared to use case 1, which has the same scaling factor for 10 EWHs, use case 4 provided a total flexibility that was 2.2 times higher, although approximately 24% less per EWH. The simulation time for use case 4 was around 18 times higher than for use case 1, and the increase in peak load compared to the baseline was similar to use case 1.

Compared to use case 2, which has a scaling factor of 2 for 10 EWHs, the total flexibility in use case 5 was 2.3 times higher, although approximately 25% less per EWH. The simulation time for use case 5 was around nine times longer than for use case 2, and the increase in peak load compared to the baseline was 3% higher than for use case 2. Figures 22 and 23 illustrate the total flexibility and aggregated power for one simulation in use case 5, where the flexibility provided was 3.6 kWh per EWH.

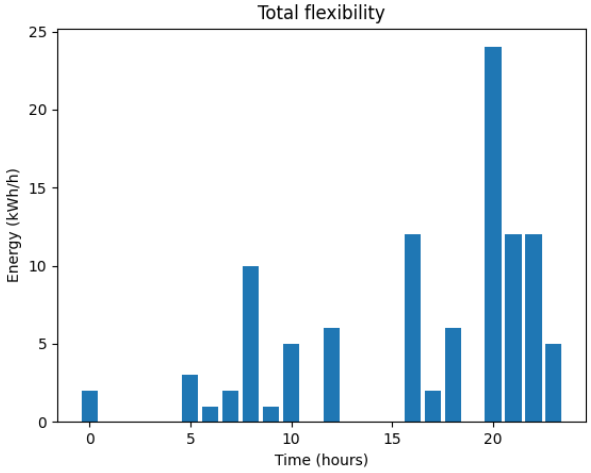

Figure 22: Hourly flexible energy for one simulation of 24 hours in use case 5 with 30 EWHs

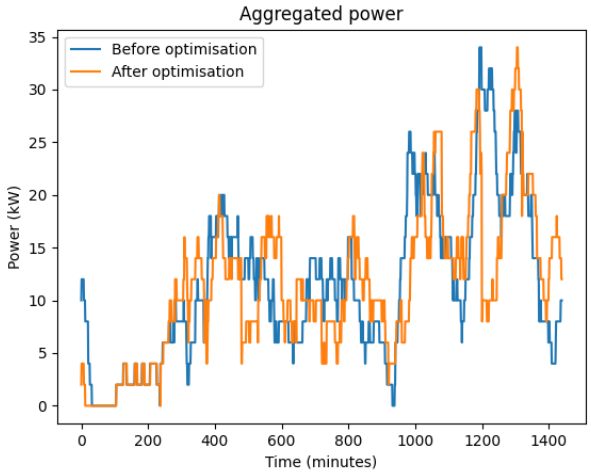

Figure 23: Aggregated power before and after optimisation for one simulation of 24 hours in use case 5 with 30 EWHs

The plots indicate that flexibility is available right from the beginning. Consequently, the aggregated power in the first hour is significantly lower than in the baseline due to the provision of flexibility from the first minute. The highest flexible power occurs around 8 pm, which is also around when the load is highest. Moreover, even though the load profile changes, the peak load remains identical to the baseline. Nevertheless, in this simulation, the peak load of over 30 kW occurs a few hours later than in the baseline.

6.1.3 Use case 6 - 100 EWHs

Use case 6 of the multi-layer GA had an average flexibility of 2.5 kWh per EWH and a maximum flexibility of 2.8 kWh per EWH, with a standard deviation of 0.2 kWh per EWH. The average simulation time was approximately 51 hours, and the average change in peak load compared to the baseline was 3%, with a standard deviation of 9%. The simulation time of over two days per simulation showcases the need for computational resources and parallel simulations when having a large number of EWHs. The total flexibility in use case 6 was 6.6 times higher than in use case 1 but 34% less per EWH. The simulation time was more than 600 times higher, and the increase in peak load compared to the baseline was 5% less than use case 1. Figures 24 and 25 display

the total flexibility and aggregated power for one simulation in use case 6, where the flexibility provided was 2.7 kWh per EWH.

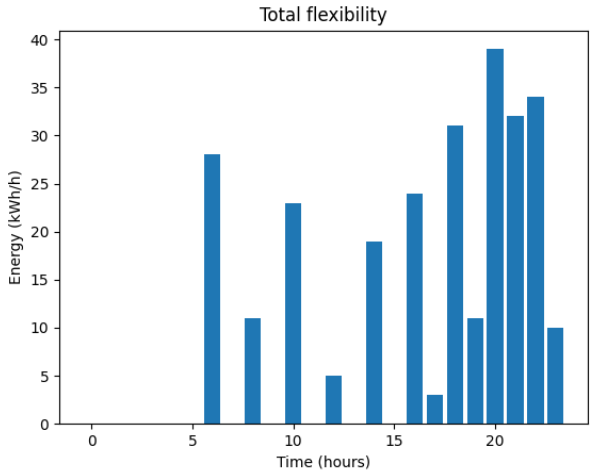

Figure 24: Hourly flexible energy for one simulation of 24 hours in use case 6 with 100 EWHs

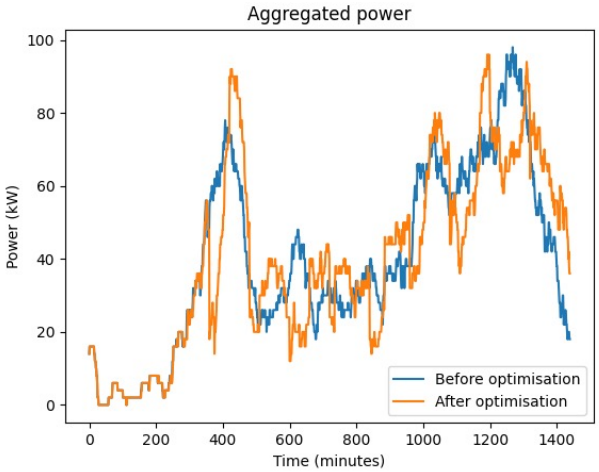

Figure 25: Aggregated power before and after optimisation for one simulation of 24 hours in use case 6 with 100 EWHs

The plots show that flexibility is provided steadily throughout the day, with a higher density in the evening. There is a shifted and increased power peak in the morning after the optimisation, showcasing the rebound issue. However, as the evening peak is delayed and reduced, the overall peak load is reduced by 2%.

6.2 Results with the multi-layer reference algorithm

Use cases 7, 8 and 9 were all run for ten simulations with 10, 30 and 100 EWHs, respectively. Table 11 presents the results from these use cases as the average, highest and standard deviation of the recorded flexible energy between the ten simulations, average simulation time and average change in peak load compared to the baseline.

Table 11: Results from use cases 7, 8 and 9 with the multi-layer reference algorithm

Use case	**Number of EWHs**	**Average flexible energy [kWh/ EWH]**	**Highest flexible energy [kWh/ EWH]**	**Standard deviationx [kWh/ EWH]**	**Average simulation time [min]**	**Average change in peak load**
7	10	3.1	3.5	0.3	< 1	11%
8	30	2.6	2.7	0.1	< 1	2%
9	100	2.4	2.6	0.1	< 1	15%

With 30 EWHs, the total flexibility was 2.5 times higher but around 16% less per EWH, and the increase in peak load was lower compared to the baseline. For the simulations with 100 EWHs, the total flexibility was 7.7 times as high as with 10 EWHs, but the average flexibility per EWH was 23% less.

Although significantly faster than the GA, as all simulations were conducted in less than a minute, the reference algorithm provided 4-30% less flexibility on average and 11-30% less for the best simulations. Additionally, the reference algorithm resulted in a higher increase in peak load than the GA for the simulations with 10 and 100 EWHs, but a lower average peak load for the simulations with 30 EWHs.

6.3 Results with the single-zone model

While use case 10 was run for 100 simulations, use cases 11-15 were all run for ten simulations. Having a significant amount of samples from use case 10, Figure 26 presents the distribution of flexibility from use case 10, which had a standard deviation of 0.1 kWh/EWH. It can be noted that all use cases here had a standard deviation of 0.1 or 0.2 kWh/EWH. Table 12 then presents the results from all use cases with the single-zone model. The results are presented as the average and highest recorded flexible energy, average simulation time and average change in peak load compared to the baseline. It can be noted that while use cases 10 and 12 with the GA used a scaling factor of 2, use case 14 had a scaling factor of 1.

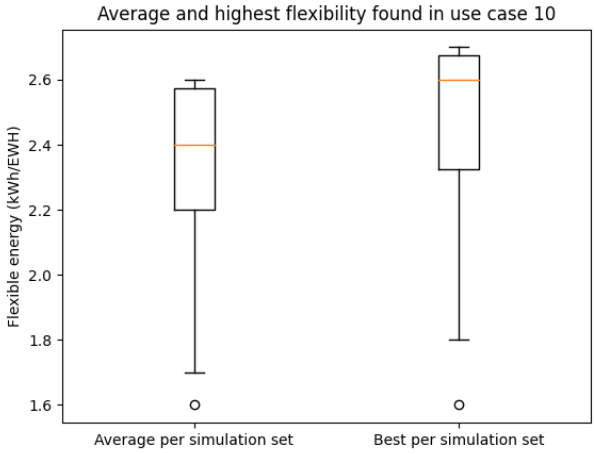

Figure 26: Results from use case 10 showing the distribution of average and best values for flexible energy per EWH. The results are presented as box plots with a box from the first to the third quartile, a vertical line representing the median, and outliers represented as dots.

Table 12: Results from use cases 10-15 with the multi-layer reference algorithm

Use case	**Number of EWHs**	**Optimisation method**	**Average flexible energy [kWh/ EWH]**	**Highest flexible energy [kWh/ EWH]**	**Average simulation time [min]**	**Average change in peak load**
10	10	GA	2.3	2.7	1	-3%
11	10	Reference algorithm	2.9	3.1	< 1	-6%
12	30	GA	2.0	2.4	23	6%
13	30	Reference algorithm	2.0	2.2	< 1	16%
14	100	GA	1.7	2.0	157	7%
15	100	Reference algorithm	1.9	2.0	< 1	8%

The results with the single-zone model suggest that the reference algorithm can find more flexibility faster than the GA, highlighting the need for an improved GA for the single-zone model. Compared to the equivalent multi-zone reference model, the single-zone model provided approximately 7-32% less flexibility on average.

6.4 Results with reconnection strategies

6.4.1 Use cases 16, 17 and 18 - 10 EWHs

Table 13 presents the results of the reconnection strategies in use cases 16-18 compared to the results of use case 2, which, similar to use cases 16-18, has a multi-layer temperature model for ten EWHs and GA with a scaling factor of 2. However, as use case 2 was run in 100 simulations and use cases 16-18 in ten, it is shown the average highest flexibility for use case 2 for a fair comparison.

Table 13: Flexible energy, simulation time and change in peak load with the reconnection strategies in use cases 16-18 compared to no reconnection strategy from use case 2 - 10 EWHs

Use case	**Reconnection strategy**	**Average flexible energy [kWh/ EWH]**	**Highest flexible energy [kWh/ EWH]**	**Standard deviation [kWh/ EWH]**	**Average simulation time [min]**	**Average change in peak load**
2	None	4.3	5.0	0.4	19	4%
16	1	4.5	5.8	0.6	20	3%
17	2	4.5	5.1	0.5	20	-6%
18	3	4.4	4.5	0.1	26	-10%

All reconnection strategies resulted in more flexibility on average than without any reconnection strategy. However, significant deviations occurred for the best simulations, ranging from 4.5 kWh per EWH for the third reconnection strategy to 5.8 kWh per EWH for the first. There were significant deviations in the average change in peak load, as the second and third reconnection strategies reduced the peak load by six and 10% on average. In comparison, the first strategy increased it by 3%, compared to a 4% increase without reconnection strategies. In contrast to the results for peak load, the results for simulation time were more consistent, around 20 minutes for strategies 1 and 2 and around 26 minutes for strategy 3. The second and third reconnection strategies provided similar average flexibility to the first strategy while simultaneously better accounting for the user

temperature comfort without increasing peak load. However, the first strategy resulted in this study's highest recorded flexibility per EWH. Figures 27 and 28 show this simulation's flexibility and power profile before and after optimisation.

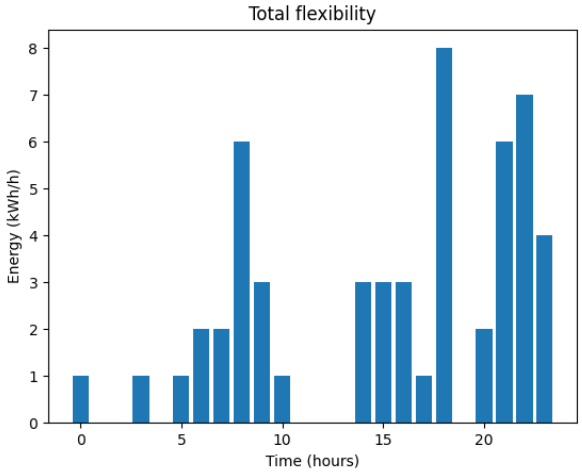

Figure 27: Hourly flexible energy for the simulation with the most flexibility for 10 EWHs using reconnection strategy 1

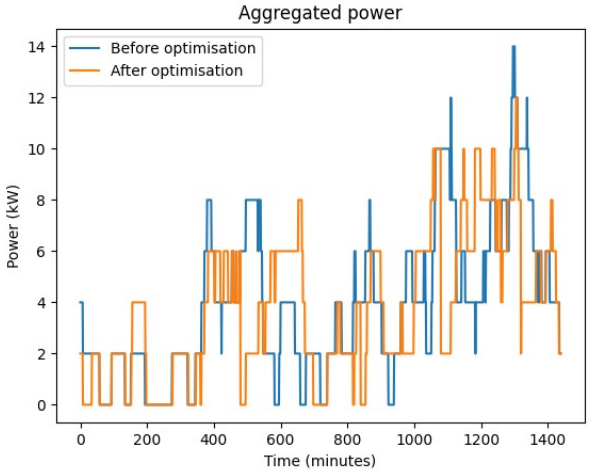

Figure 28: Aggregated power before and after optimisation for the simulation with the most flexibility for 10 EWHs using reconnection strategy 1

For this simulation, flexibility was found in most hours of the day, including the first and last hour, and distinct peak flexible energy was found at around 8 am, 6 pm and 10 pm. It can also be seen that the peak load was reduced from 14 kW to 12 kW, meaning that 6 of 10 EWHs were turned on simultaneously after the optimisation compared to 7 of 10 before the optimisation.

6.4.2 Use cases 19, 20 and 21 - 30 EWHs

Table 14 presents the results of the reconnection strategies in use cases 19-21 compared to the results of the fifth use case, which, similar to use cases 19-21, has a multi-layer temperature model for 30 EWHs and GA with a scaling factor of 2.

Table 14: Flexible energy, simulation time and change in peak load with the reconnection strategies in use cases 19-21 compared to no reconnection strategy in use case 5 - 30 EWHs

Use case	**Reconnection strategy**	**Average flexible energy [kWh/ EWH]**	**Highest flexible energy [kWh/ EWH]**	**Standard deviation [kWh/ EWH]**	**Average simulation time [min]**	**Average change in peak load**
5	None	3.2	3.8	0.2	187	7%
19	1	3.6	4.3	0.5	263	4%
20	2	3.4	3.9	0.3	253	2%
21	3	3.2	3.6	0.3	293	4%

On average, the use cases with reconnection strategies and 30 EWHs offered equal or more flexibility than the simulations without reconnection strategy. The simulation time was approximately 4-5 hours with reconnection strategies and 3 hours without reconnection strategies. Moreover, all reconnection strategies resulted in lower peak load, with an average increase ranging from 2% to 4%, compared to 7% without reconnection strategies. While the second and third strategies provided less flexibility than the first, they also considered user temperature comfort better without increasing peak load more.

6.4.3 Use cases 22, 23 and 24 - 100 EWHs

Table 15 presents the average and highest flexible energy, average simulation time and average change in peak load of the reconnection strategies in use cases 22-24. Table 15 also includes the results of the sixth use case, which, similar to use cases 22-24, has a multi-layer temperature model for 100 EWHs and GA with a scaling factor of 1.

Table 15: Flexible energy, simulation time and change in peak load with the reconnection strategies in use cases 22-24 compared to no reconnection strategy in use case 6 - 100 EWHs

Use case	**Reconnection strategy**	**Average flexible energy [kWh/ EWH]**	**Highest flexible energy [kWh/ EWH]**	**Standard deviation [kWh/ EWH]**	**Average simulation time [min]**	**Average change in peak load**
6	None	2.5	2.8	0.2	3052	3%
19	1	2.5	2.7	0.3	2821	8%
20	2	2.5	2.5	0.2	2811	3%
21	3	2.5	2.8	0.2	2626	3%

All reconnection strategies provided equal average flexibility compared to case 6 without a reconnection strategy. Moreover, the first and third reconnection strategies and use case 6 without reconnection strategy all produced an equal change in peak load of 3%, while reconnection strategy 2 provided an 8% increase.

6.5 Applying mFRR-prices

Different numbers for the aggregator's revenue in the mFRR-market can be found when applying the three price scenarios to the flexibility. Using the average and best values for 10, 30 and 100 EWHs of all results, Figure 29 depicts the potential market revenue for the aggregator. The average and best values for 10 EWHs are 4.5 and 5.8 kWh per EWH per day, for 30 EWHs are 3.5 and 4.3 kWh per EWH per day and for 100 EWHs are 2.5 and 2.8 kWh per EWH per day.

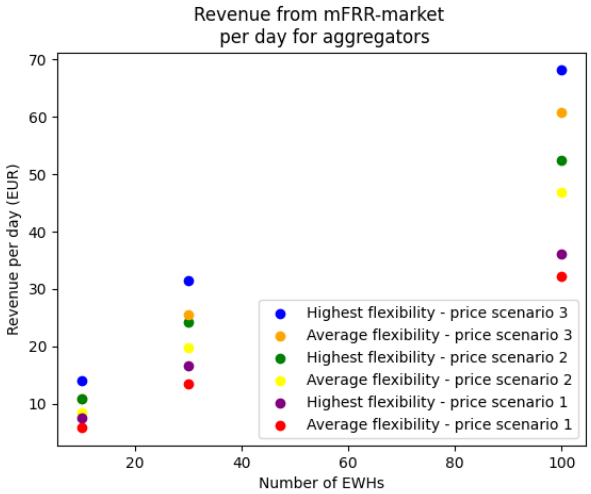

Figure 29: Average and highest potential revenue per day from the mFRR-market for the aggregator - using three price scenarios and 10, 30 and 100 EWHs

With 10 EWHs, the aggregator can expect to make 5-15 EUR daily, depending on the price scenario. For price scenario 1 with average prices, the aggregator can expect to make 5.0-7.5 EUR depending on if the average or highest flexibility from the simulations is used. The aggregator can expect to make 8.5-11.0 EUR daily for the second scenario with volatile prices. However, for the volatile price scenario, this depends strongly on how flexibility is provided throughout the day.

The aggregator can expect to make around five EUR per day if all flexibility is provided in the hour with the lowest price. With 30 EWHs in the portfolio, the aggregator can expect to make 10-30 EUR daily. Lastly, with 100 EWHs in the portfolio, the revenue is even more uncertain but can be expected to be around 30-70 EUR daily for the aggregator, depending on the price scenario.

6.6 Summary of results

This section primarily summarises the results for the different use cases, distinguishing between the simulations using 10, 30 and 100 EWHs. Then, the results for different numbers of EWHs are compared. The comparisons show the used temperature model, optimisation method and thereunder scaling of the GA when used, achieved flexible energy, average simulation time and average change in peak load compared to the baseline.

The 24 use cases resulted in varying degrees of flexibility, simulation times and changes in peak load. The average daily flexibility per EWH ranged from 1.7 to 4.4 kWh, depending on the use case. Some use cases provide significantly more flexibility than others but often at the cost of longer simulation times. The average increase in peak load compared to the baseline ranged from -3% to 16%, depending on the use case.

6.6.1 Results with 10 EWHs

Table 16 shows the results for 10 EWHs with the different methods in this work. Then, Figure 30 presents achieved flexible energy, best and average, for the use cases with multi-layer temperature modelling, compared to the simulation times used to achieve this flexibility.

Table 16: An overview of flexible energy, simulation time and change in peak load for the considered methods and models - 10 EWHs

Model	**Method**	**Scaling**	**Average flexible energy [kWh/ EWH]**	**Highest average flexible energy [kWh/ EWH]**	**Highest flexible energy [kWh/ EWH]**	**Average simulation time [min]**	**Average change in peak load**
Multi -layer	GA	3	4.4	5.0	5.4	42	5 %
Multi -layer	GA	2	4.3	5.0	5.3	19	4 %
Multi -layer	GA	1	3.8	4.4	4.8	5	8 %
Multi -layer	Reference algorithm	-	3.1	-	3.5	< 1	11 %
Single -zone	Reference algorithm	-	2.9	-	3.1	< 1	-6 %
Single -zone	GA	2	2.3	2.4	2.7	1	-3 %

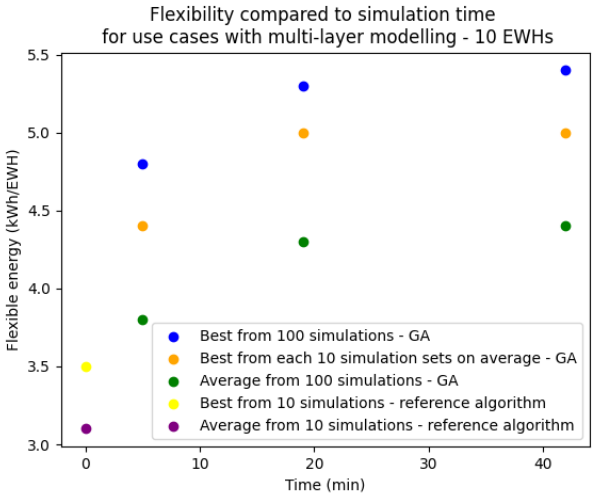

Figure 30: Flexible energy per EWH per simulation time and number of simulations with scaling factors of 1, 2 and 3 in the GA - 10 EWHs

For 10 EWHs, use case 3 provided the highest average flexibility. Use case 2 also showed promising results, with 0.1 kWh per EWH less average flexibility than use case 3 but with less than half of the average simulation time. The other use cases with 10 EWHs provided less flexibility than use cases 2 and 3 but with shorter simulation times. Using the GA, the use cases with longer simulation times generally provided higher flexibility without increasing the peak load. It is also evident that the simulations with a multi-layer model provide significantly more flexibility than a single-zone model but at the expense of increased peak load.

6.6.2 Results with 30 EWHs

Table 17 shows the results for 30 EWHs for the different methods in this work. Then, Figure 31 presents achieved flexible energy, best and average, for the use cases with multi-layer modelling, compared to the simulation times used to achieve this flexibility.

Table 17: An overview of flexible energy, simulation time and change in peak load for the considered methods and models - 30 EWHs

Model	**Method**	**Scaling**	**Average flexible energy [kWh/ EWH]**	**Highest flexible energy [kWh/ EWH]**	**Simulation time [min]**	**Change in peak load**
Multi-layer	GA	2	3.2	3.8	187	7 %
Multi-layer	GA	1	2.9	3.3	73	4 %
Multi-layer	Reference algorithm	-	2.6	2.7	< 1	2 %
Single-zone	Reference algorithm	-	2.0	2.4	< 1	6 %
Single-zone	GA	2	2.0	2.2	23	16 %

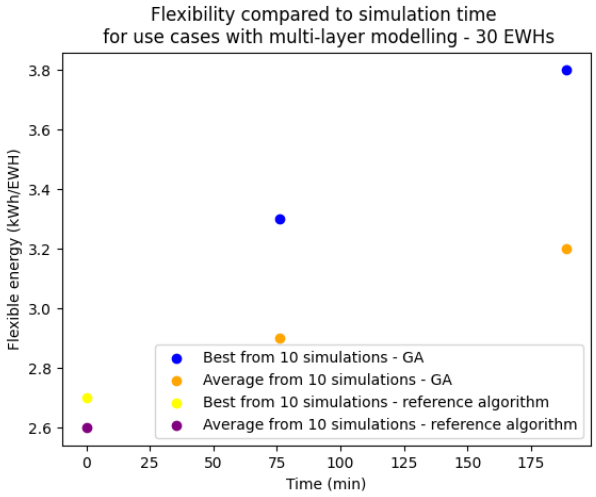

Figure 31: Flexible energy per EWH per simulation time and number of simulations with scaling factors of 1 and 2 in the GA - 30 EWHs

The results for 30 EWHs show a wide range of flexibility from the different use cases. The best results were achieved in use case 5 with the GA and multi-layer model, achieving the highest average and best flexibility. Further, the simulation time varied significantly, with some use cases taking less than a minute to complete while use case 5 required several hours. Opposite from the results with 10 EWHs, the single-zone model here provides a much-increased peak load, being 16% on average with the GA.

6.6.3 Results with 100 EWHs

Table 18 shows the average results for 100 EWHs for the different methods in this work. Then, Figure 32 presents achieved flexible energy, best and average, for the use cases with multi-layer modelling, compared to the simulation times used to achieve this flexibility.

Table 18: An overview of flexible energy, simulation time and change in peak load for the considered methods and models - 100 EWHs

Model	**Method**	**Scaling**	**Average flexible energy [kWh/ EWH]**	**Highest flexible energy [kWh/ EWH]**	**Simulation time [min]**	**Change in peak load**
Multi-layer	GA	1	2.5	2.8	3052	3 %
Multi-layer	Reference algorithm	-	2.4	2.5	< 1	15 %
Single-zone	Reference algorithm	-	1.9	2.0	< 1	8 %
Single-zone	GA	1	1.7	2.0	157	7 %

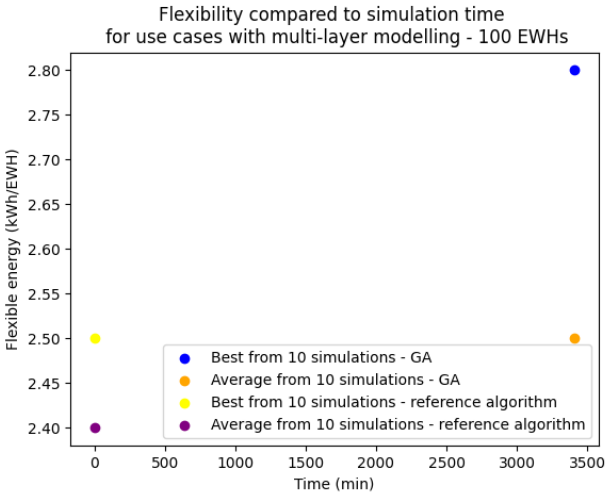

Figure 32: Flexible energy per EWH per simulation time and number of simulations with a scaling factor of 1 in the GA - 100 EWHs

With 100 EWHs, the GA achieved the most flexible energy with the multi-layer model and the lowest increase in peak load. However, its simulation time was around 51 hours. The reference algorithm found only 0.1 kWh/EWH less flexibility on average but with a simulation time of less than a minute. On the downside, the reference algorithm had a 15% average increase in peak load, compared to 3% for the GA.

6.6.4 Results with reconnection strategies

For 10, 30 and 100 EWHs represented, all reconnection strategies resulted in higher than or equal average flexibility compared to the simulations without reconnection strategies. Simultaneously, reconnection strategies 2 and 3 reduced the peak load substantially compared to the first reconnection strategy and without reconnection strategies for the simulations with 10 and 30 EWHs in the portfolio. The reconnection strategies achieved these results while simultaneously managing cold-load pick-ups but with the drawback of an increased risk of cold water for consumers.

6.6.5 Results with mFRR-prices

When applying mFRR-prices to the obtained flexibility, the revenue for aggregators can be estimated. Although the total flexibility, and thus revenue, increases with the number of EWHs, the

flexibility and thus revenue per EWH decreases with the number of EWHs. Depending on the price scenarios and the number of EWHs in the portfolio, this work estimates that an aggregator can expect a revenue of 0.3 to 1.5 EUR per EWH per day.

7 Discussion

The discussion primarily addresses the main factors impacting the optimisation results, including the number of EWHs in the portfolio, choice of temperature models and optimisation methods, reconnection strategies and values of parameters. Secondarily, the discussion addresses the challenges of applying the methods in the real world for aggregators.

In this case study, the number of EWHs greatly impacted the achieved flexibility, where the use cases involving 100 EWHs provided more aggregated flexibility and less per EWH. The significant difference in flexibility per EWH between the simulations with a different number of EWHs can be explained by the minimum bid size constraint requiring 10% of the portfolio to bid simultaneously. While this requires only one EWH to bid when having ten EWHs in the portfolio, it requires ten EWHs to bid with 100 EWHs in the portfolio, thus losing out on flexibility when having nine or fewer EWHs being possible to bid. In addition to less flexibility and revenue per EWH, significantly longer simulation times were required for the use cases with many EWHs, exponentially increasing with the number of EWHs using the GA. However, when using the reference algorithm, all simulations were completed within one minute, and the simulation time increased linearly with the number of EWHs.

Multi-layer temperature modelling yielded significantly more flexibility than single-zone temperature modelling. The number of feasible bids per iteration may be one of the reasons why the simulations with the multi-layer model outperformed the simulations with a single-zone model in finding flexibility. Moreover, the number of feasible bids per iteration in the simulations was particularly decisive when using the GA, as the numbers of generations and individuals per generation in the GA were chosen proportional to the number of feasible bids. While the EWHs were found to be turned on 17% of the time with the single-zone model, the multi-layer model found, with higher accuracy, that the EWHs were turned on 20% of the time, using the same input data as with the single-zone model. Consequently, the numbers of feasible bids were significantly lower for the simulations using the single-zone model. It was, therefore, less flexible energy to extract in the simulations using the single-zone model. Additionally, as the numbers of generations and individuals per generation in the GA were set proportional to the number of feasible bids, the GA was less powerful for the simulations with the single-zone model.

Using the multi-layer model, the GA outperformed the reference algorithm in finding flexibility for the simulations with 10 and 30 EWHs in the portfolio. However, with 100 EWHs in the portfolio, the GA only found 0.1 kWh more per EWH per day, but at the expense of a 51-hour longer average simulation time. One of the reasons why the GA lacks performance with 100 EWHs in the portfolio is the use of a scaling factor of one, compared to two with 10 and 30 EWHs in the portfolio. Additionally, having a larger number of EWHs in the portfolio increases the number of attributes per individual in the GA, expanding the algorithm's search space and making it more difficult for the GA to find optimal solutions.

Moreover, the results show that reconnection strategies can provide more flexibility and better manage cold load pick-ups for the load from EWHs, compared to the use cases without reconnection strategies. Additionally, reconnection strategies 2 and 3 resulted in significantly lower peak load for the simulations with 10 and 30 EWHs in the portfolio than those without reconnection strategies. The use cases with reconnection strategies may have performed better than those without because of a different number of feasible bids and thus generations and individuals per generation in the GA or because of the randomness in the GA.

The reconnection strategies also have some downsides. On average, the simulations with reconnection strategies took longer to finish than those without for the use cases with 10 and 30 EWHs, particularly with the third reconnection strategy. The difference in computational performance might have come from the complexity of recalculating temperatures when applying the third reconnection strategy, which also considers the hot water usage for the next 30 minutes. However, for 100 EWHs, the simulations with reconnection strategies took, on average, a shorter time than those without, despite being more complex. This difference in computational performance indic-

ates that the randomness of the GA and the performance of the assigned computational resources are more decisive factors in the simulation times than the computational complexity of the reconnection strategies. Another potential issue with the reconnection strategies used in this work is the possibility of violating the comfort temperature of the consumers outside the bidding periods. As the strategies used in this work do not minimise the risk of cold water for the consumers, they do not guarantee that the temperature in the EWHs remains within the comfort range.

Outside of the reconnection strategies, reducing peak load and managing rebound effects were not prioritised. However, the problem could have gotten different results if this had been a more significant part of the problem. On the downside, making more room for peak load reduction could have limited the flexibility extracted from the EWHs, as flexibility maximisation would have been given less consideration.

How the EWHs were modelled was likely decisive for the problem's results. First and foremost, hot water usage is decisive because it is the primary input data and input uncertainty for the problem. Additionally, the EWHs were modelled homogeneously by having identical physical parameters. Using a heterogeneous portfolio of EWHs could have yielded different results. Moreover, changing the setpoint for the temperatures and placement of the heating element and thermostat might provide a different amount of flexibility, as these considerations involve significant uncertainty and are not optimised to maximise flexibility.

Computational efficiency could have been prioritised differently. While this work used a fourth-order Runga Kutta method to solve the initial value problem of constraint (1), a simpler method, such as Euler's method, would have solved the problems faster but at the expense of less accuracy. Similarly, using fewer than ten layers in the multi-layer modelled would have lowered the algorithm's simulation time but been less accurate. However, for this work, as indicated in Figures 9, 10 and 11, and Table 8, the temperatures in the top layers were for most minutes identical, so fewer layers could have been used without significantly reducing the accuracy of the modelling.

Lastly, the choice of parameters could have been decisive for the results. The length of the bidding period, the period in which the GA is applied in the iterative approach, and the planning horizon for the problem could have been particularly decisive, as these parameters were not optimised. Although the results of this work show that a 15-minute bidding period can provide significant flexibility, more flexibility can be provided with more frequent bidding periods, for example, one minute. That would mean each EWH can provide flexibility in parts of each 15-minute bidding period and not be limited to providing for the entire 15-minute bidding period. On the downside, this change could require more computational resources for the aggregator. For the simulations using the GA, a shortened time period could have taken away the GA's ability to optimise flexibility concerning the minimum bid size constraint. On the other hand, an extended time period could lead to losing the optimal choice of flexibility from each EWH within each period. Lastly, extending the planning horizon beyond 24 hours would provide a better understanding of the dynamics of flexibility provision over a longer time. However, this would also require more computational resources. Furthermore, extending the planning horizon beyond 24 hours could result in less average daily flexibility as some EWHs must complete a heating cycle over midnight before bidding the next day and thus have less time to bid the next day.

A real-world implementation of flexibility from EWHs requires consideration of additional factors not explored in this work. For example, aggregators might be concerned with backup resources and risk management. Furthermore, implementing real-world solutions requires further integration towards the regulations and markets. For example, market rules can determine the minimum bid size to be submitted, significantly determining the flexibility potential. Additionally, computation time is essential for the aggregator's ability to act in the market, as it cannot initiate actions as planned if its algorithm takes too long to run and can therefore lose out on revenue. Finally, implementing real-world solutions must consider the computational resources required to solve the optimisation problem with significant uncertainty of the computational cost. For example, the number of EWHs for the aggregator can be higher than that considered in this study, which can determine the computational resources required for the aggregator. In practice, aggregators must consider the trade-off between the level of flexibility achieved and the computational resources

required to achieve it.

8 Conclusion

This thesis investigates the potential of EWHs as flexible energy resources for the power grid by maximising the aggregated flexibility of the EWHs. A comprehensive theoretical framework identifies the non-linear temperature behaviour of EWHs, technical challenges and barriers for aggregators, and relevant optimisation techniques for problems concerning EWHs. The literature review then reveals that most of the previous literature has aimed to control a single EWH or used inaccurate temperature modelling for groups of EWHs, thus establishing a research gap in the modelling of EWHs. By assessing three pillars for aggregators with EWHs, namely modelling, market participation and optimisation, this work highlights opportunities and challenges for market-participating aggregators with EWHs.

To accurately maximise the flexibility provided by the aggregator, this work uses a 10-layer stratified model with a one-minute resolution for up to 100 EWHs. The EWHs are assumed to be part of an aggregator's portfolio of flexible resources applied in an mFRR-market directly from the aggregator or through a third party. A genetic algorithm and a reference algorithm are created from scratch and employed to handle the non-linear behaviour of the EWHs, aiming to achieve a good trade-off between flexibility maximisation, accurate modelling, and computational efficiency. Furthermore, three different reconnection strategies are implemented to manage the simultaneous aggregated load from EWHs.

The results demonstrate that aggregators can provide up to 5.8 kWh of flexibility per EWH per day, translating to potential revenue of up to 1.5 EUR per day per EWH based on mFRR-prices in NO1 from January 2023. A genetic algorithm with a multi-layer temperature model provides the most flexibility of the methods in this work while simultaneously modelling the EWHs accurately. However, the simulation time of the GA scales poorly for many aggregated EWHs. In comparison, the simplified reference algorithm is fast for all numbers of EWHs and might therefore be more suitable for aggregators with many EWHs in their portfolio. Additionally, all implemented reconnection strategies yielded higher or equal average flexibility compared to simulations without reconnection strategies while addressing the issue of the simultaneous connection of EWHs, but with an increased risk of cold water for the consumers.

Several factors are essential for the optimisation results of this work and for the applicability of EWH flexibility in real life for aggregators. The flexibility per EWH decreased substantially with the number of EWHs in the portfolio, primarily based on how the minimum bid size constraint is formulated in the optimisation problem and due to the increased search space in the GA occurring when scaling the problem size. Moreover, the choice of values for parameters, thereunder the parameters in the GA, were not tuned for optimal performance. Therefore, this should be addressed in future research to maximise flexibility from EWHs using a GA. In practice, aggregators face additional challenges, like risk management and computational uncertainty, which must be adequately addressed to employ EWHs as flexible resources in the power grid.

9 Future work

Several aspects of this master's thesis have significant potential for further investigation. The GA can be improved, and its parameters and penalisations can be tuned to achieve better performance. In addition, there is great potential for future research based on this work's modelling of EWHs, market participation and optimisation, and the prioritisation of stochasticity and uncertainty. This chapter presents how these areas can be addressed in future research.

The main shortcoming of this work is the remaining potential for exploration of the GA, combined with the need for optimal turning of the parameters and penalisations. By using a different type of GA, or an improved version of the penalty-based GA of this work, future research can aim to achieve faster simulation times and better scalability of the method for a larger number of EWHs in the aggregator's portfolio. Moreover, as the parameters in the GA must be tuned to achieve optimal performance, future work can systematically tune and optimise parameters and penalisation for the different use cases and each optimisation period in the planning horizon.

Moreover, future research can investigate a hybrid of the multi-layer and single-zone temperature models, combining the multi-layer model's accuracy and performance with the single-zone model's computational efficiency. While the multi-layer model provides a more detailed representation of the system, its high computational cost may limit its practical applications, especially at scale. On the other hand, the single-zone model is computationally efficient but does not accurately capture the EWHs' temperature dynamics. By integrating the strengths of both models, it may be possible to develop more efficient and accurate modelling. The GA could, for example, use the single-zone model for the optimisation and the multi-layer model outside of the optimisation.

Future research can also apply the methods to different markets. The study assumes that the EWHs are flexible resources in an mFRR-market, applying three different price scenarios to the obtained flexibility. However, there are other markets where EWHs can provide flexibility, such as frequency containment reserve markets or local flexibility markets. Additionally, other price scenarios and revenue calculations can be used.

Future research can solve the problem with other suitable metaheuristic methods. While this study compares the performance of the GA to the simplified reference algorithm, other methods, such as PSO, might solve this problem more efficiently. Another potential for future work within optimisation is expanding the problem to include electricity costs in the objective function. Then, aggregators can utilise their assets efficiently by offering electricity cost reduction as an additional service to their customers with EWHs.

At last, future work should address uncertainty and stochasticity to provide helpful insight for aggregators. While uncertainty can be addressed by investigating computational uncertainty in more detail, stochasticity can be addressed by applying stochastic variables in the optimisation problem. In addition, experimenting with other values for parameters and input data can provide aggregators with more insight into the flexibility potential of their assets.

Bibliography

[1] E. Vabø. 'Operation of electric water heaters for aggregators'. In: (2022). Specialisation Project Report, TET4510, Department of Electric Energy, Norwegian University of Science and Technology (NTNU), Trondheim.

[2] UN. *The Paris Agreement*. Accessed: 2022-28-09. URL: https://unfccc.int/process-and-meetings/the-paris-agreement/the-paris-agreement.

[3] ACER. *About the Green Deal*. Accessed: 2022-28-09. URL: https://www.acer.europa.eu/green-deal/about-green-deal.

[4] H. Vefsnmo et al. *Scenarier for fremtidens elektriske distribusjonsnett anno 2030-2040*. Accessed: 2022-12-02. Jan. 2020. URL: https://sintef.brage.unit.no/sintef-xmlui/bitstream/handle/11250/2681944/01-2020%5C%2B-%5C%2BCINELDI-rapport.pdf?sequence=2&isAllowed=y.

[5] G. C. Gissey et al. 'Value of energy storage aggregation to the electricity system'. In: *Energy Policy* 128 (2019), pp. 685–696.

[6] Statnett. *Distributed balancing of the power grid*. Accessed: 2022-11-25. Feb. 2021. URL: https://www.statnett.no/contentassets/5f177747331347f1b5da7c87f9cf0733/2021.02.24-results-from-the-efleks-pilot-in-the-mfrr-market--.pdf.

[7] H. Saele and O. S. Grande. 'Demand Response From Household Customers: Experiences From a Pilot Study in Norway'. In: *IEEE Transactions on Smart Grid* 2.1 (2011), pp. 102–109.

[8] Energikommisjonen. *Mer av alt – raskere*. Feb. 2023. URL: https://www.regjeringen.no/no/dokumenter/nou-2023-3/id2961311/?ch=1.

[9] M. B. Ryssdal et al. *Value of flexibility from electrical storage water heaters*. Accessed: 2022-11-09. Feb. 2020. URL: https://thema.no/wp-content/uploads/TE-2020-17-Value-of-flexibility-from-electrical-storage-water-heaters-corrected-1.pdf.

[10] E. Hillberg et al. *Flexibility needs in the future power system*. Accessed: 2022-12-12. Mar. 2019. URL: https://www.iea-isgan.org/wp-content/uploads/2019/03/ISGAN_DiscussionPaper_Flexibility_Needs_In_Future_Power_Systems_2019.pdf.

[11] M. Shaad et al. 'Parameter identification of thermal models for domestic electric water heaters in a direct load control program'. In: *2012 25th IEEE Canadian Conference on Electrical and Computer Engineering (CCECE)*. 2012.

[12] ENTSO-E. *ENTSO-E's Response to the European Commission Public Consultation on Electricity Market Design*. Accessed: 2023-05-20. Feb. 2023. URL: https://www.entsoe.eu/news/2023/02/14/entso-e-response-to-the-european-commission-public-consultation-on-electricity-market-design/.

[13] L. Brouyaux et al. 'Chance-Constrained Frequency Containment Reserves Scheduling with Electric Water Heaters'. In: *2021 IEEE PES Innovative Smart Grid Technologies Europe (ISGT Europe)*. 2021.

[14] W. Zhaojun et al. *Proceedings of the 11th International Symposium on Heating, Ventilation and Air Conditioning (ISHVAC 2019)*. Springer Singapore, 2020, p. 78.

[15] M. Pied, M. F Anjos and R. P Malhamé. 'A flexibility product for electric water heater aggregators on electricity markets'. In: *Applied Energy* 280 (2020), p. 115168.

[16] M. Zuñiga et al. 'Parameter estimation of electric water heater models using extended Kalman filter'. In: *IECON 2017 - 43rd Annual Conference of the IEEE Industrial Electronics Society*. 2017, pp. 386–391.

[17] OSO. *Varmtvannsbereder SAGA STANDARD - S*. Accessed: 2022-11-09. URL: https://osohotwater.no/product/%20varmtvannsbereder-saga-standard/.

[18] V. Lakshmanan, H. Sæle and M. Degefa. 'Electric water heater flexibility potential and activation impact in system operator perspective – Norwegian scenario case study'. In: *Energy* 236 (2021), p. 121490.

[19] OSO. *Industrial OEM Solutions*. Accessed: 2023-06-06. URL: https://osohotwater.no/oem-stainless-steel-tanks/.

[20] OSO. *Produkter*. Accessed: 2022-11-09. URL: https://www.osoenergy.no/produkter/.

[21] ENOVA. *Smart varmtvannsbereder*. Accessed: 2022-11-09. URL: https://www.enova.no/privat/alle-energitiltak/smart-varmtvannsbereder/.

[22] S. Jørgensen. *Smarte varmtvannsberedere fikk Smartgridsenterets innovasjonspris 2022*. Accessed: 2022-11-09. URL: https://ide-smartgrids.no/nyheter/smarte-varmtvannsberedere-fikk-smartgridsenterets-innovasjonspris-2022/.

[23] J. Gao et al. 'A feasibility study of automated plug-load identification from high-frequency measurements'. In: *2015 IEEE Global Conference on Signal and Information Processing (GlobalSIP)*. 2015, pp. 220–224.

[24] J. Rajasekharan and S. V. Pandiyan. 'Recursive training based physics-inspired neural network for electric water heater modeling'. In: *Energy informatics* 5 (2022), p. 58.

[25] The Engineering ToolBox. *Water - Density, Specific Weight and Thermal Expansion Coefficients*. Accessed: 2022-11-09. URL: https://www.engineeringtoolbox.com/water-density-specific-weight-d_595.html.

[26] Energy Education. *Specific heat capacity*. Accessed: 2022-11-09. URL: https://energyeducation.ca/encyclopedia/Specific_heat_capacity.

[27] US Department of Energy. *Sizing a New Water Heater*. Accessed: 2023-06-06. URL: https://www.energy.gov/energysaver/sizing-new-water-heater.

[28] Commercial Washrooms. *How Much Water Does A Low Flow Shower Head Save?* Accessed: 2022-11-09. URL: https://www.commercialwashroomsltd.co.uk/blog/knowledgebase-faqs/how-much-water-does-a-low-flow-shower-head-save.html.

[29] V. Kapsalis and L. Hadellis. 'Optimal operation scheduling of electric water heaters under dynamic pricing'. In: *Sustainable Cities and Society* 31 (Feb. 2017).

[30] L. Qiong et al. 'Business strategies for flexibility aggregators to steer clear of being "too small to bid"'. In: *Renewable and Sustainable Energy Reviews* 143 (2021), p. 110908.

[31] P. Kepplinger. 'Autonomous Demand Side Management of Domestic Hot Water Heaters'. PhD thesis. 2018.

[32] Carolina Knowledge Center. *Newton's Law of Cooling*. Accessed: 2022-11-09. URL: https://knowledge.carolina.com/physical-science/physics/newtons-law-of-cooling/.

[33] M. Alvarez et al. 'Demand Response Strategy Applied to Residential Electric Water Heaters Using Dynamic Programming and K-Means Clustering'. In: *IEEE Transactions on Sustainable Energy* 11.1 (2020), pp. 524–533.

[34] P. Kepplinger et al. 'State estimation of resistive domestic hot water heaters in arbitrary operation modes for demand side management'. In: *Thermal Science and Engineering Progress* 9 (2019), pp. 94–109.

[35] M. Degefa, I. B. Sperstad and H. Sæle. 'Comprehensive classifications and characterizations of power system flexibility resources'. In: *Electric Power Systems Research* 194 (2021).

[36] A. M. A. Ahmed et al. 'Potential Energy Flexibility for a Hot-Water Based Heating System in Smart Buildings via Economic Model Predictive Control'. In: *2017 International Symposium on Computer Science and Intelligent Controls (ISCSIC)*. 2017, pp. 1–5.

[37] N Damsgaard et al. 'Study on the effective integration of Distributed Energy Resources for providing flexibility to the electricity system: Final report to The European Commission'. In: *Final Rep. to Eur. Comm.* (2015), p. 179.

[38] D. Stølsbotn. *Hvilken teknologi bruker et fleksibelt, intelligent, robust og kostnadseffektivt nett i 2040? Presentation at CINELDI open day 2022, Scandic Nidelva*. Nov. 2022.

[39] R. Verhaegen and C. Dierckxsens. 'Existing business models for renewable energy aggregators'. In: *linea]. Disponible en: http://bestres. eu/wp-content/uploads/2016/08/BestRES Existing-business-models-for-RE-aggregators. pdf* 246 (2016).

[40] M. Kubli and P. Canzi. 'Business strategies for flexibility aggregators to steer clear of being "too small to bid"'. In: *Renewable and Sustainable Energy Reviews* 143 (2021), p. 110908.

[41] H. Sæle. *Fleksibilitet og interaksjon DSO/TSO - presentation at CINELDI open day 2022, Scandic Nidelva*. Nov. 2022.

[42] V. F. Landmark. *Fleksibilitetsmarked fortsatt på pilotstadiet - kreves det regulatoriske grep? The Smart Grid Conference 2022, Scandic Hell Værnes*. Sept. 2022.

[43] I. Lampropoulos et al. 'A system perspective to the deployment of flexibility through aggregator companies in the Netherlands'. In: *Energy Policy* 118 (2016), pp. 534–551.

[44] N. Saker, M. Petit and J.L. Coullon. 'Demand side management of electrical water heaters and evaluation of the Cold Load Pick-Up characteristics (CLPU)'. In: *2011 IEEE Trondheim PowerTech*. 2011, pp. 1–8.

[45] A. Ersdal et al. 'Model predictive load–frequency control taking into account imbalance uncertainty'. In: *Control Engineering Practice* 53 (2015).

[46] Statnett. *Tertiærreserver*. Accessed: 2022-11-09. Oct. 2018. URL: https://www.statnett.no/for-aktorer-i-kraftbransjen/systemansvaret/kraftmarkedet/reservemarkeder/tertiarreserver/.

[47] Statnett. *Nytt automatisert mFRR-marked*. Accessed: 2022-11-09. June 2021. URL: https://www.statnett.no/for-aktorer-i-kraftbransjen/systemansvaret/kraftmarkedet/reservemarkeder/tertiarreserver/nytt-automatisert-mfrr-marked/.

[48] ENTSO-E. *Manually Activated Reserves Initiative*. Accessed: 2023-05-20. URL: https://www.entsoe.eu/network_codes/eb/mari/.

[49] USEF. *Recommended practices for DR market design*. Accessed: 2022-11-09. Sept. 2017. URL: https://www.usef.energy/app/uploads/2017/09/Recommended-practices-for-DR-market-design-2.pdf.

[50] NODES. *Market design*. Accessed: 2023-05-20. URL: https://nodesmarket.com/market-design/.

[51] NODES. *NorFlex project demonstrate integration to Statnett's mFRR market*. Accessed: 2023-05-20. URL: https://nodesmarket.com/norflex-project-demonstrate-integration-to-statnetts-mfrr-market/.

[52] S. Ø. Ottesen, M. Haug and H. Nygård. 'A Framework for Offering Short-Term Demand-Side Flexibility to a Flexibility Marketplace'. In: *Energies* 13 (2020), p. 3612.

[53] J. Xiaolong, W. Qiuwei and J. Hongjie. 'Local flexibility markets: Literature review on concepts, models and clearing methods,' in: *Applied Energy* 261 (2020), p. 11487.

[54] Gurobi. *Mixed-Integer Programming (MIP)- A Primer on the Basics*. Accessed: 2023-05-20. URL: https://www.gurobi.com/resources/mixed-integer-programming-mip-a-primer-on-the-basics/.

[55] Statnett. *Vilkår for tilbud, aksept, aktivering og prising i aktiveringsmarkedet for mFRR (regulerkraftmarkedet)*. Accessed: 2022-11-09. Jan. 2022. URL: https://www.statnett.no/globalassets/for-aktorer-i-kraftsystemet/systemansvaret/retningslinjer---horinger/vilkar-mfrr-gjeldende-fra-1.1.2022-inkl-overgangsfase-.pdf.

[56] J. Nocedal and S. J. Wright. *Numerical Optimization*. 2e. Springer, 2006.

[57] M. Wu et al. 'Multi-objective optimization for electric water heater using mixed integer linear programming'. In: *Journal of Modern Power Systems and Clean Energy* 7.5 (2019), pp. 1256–1266.

[58] K. Sørensen and F. Glover. *Metaheuristics 3rd edition*. Springer London, 2013, pp. 960–970.

[59] C.Blom and A. Roli. 'Metaheuristics in Combinatorial Optimization: Overview and Conceptual Comparison'. In: *ACM Comput. Surv.* 35 (2001), pp. 268–308.

[60] S. Luke. *Essentials of Metaheuristics*. Accessed: 2023-06-06. 2016. URL: https://cs.gmu.edu/~sean/book/metaheuristics/Essentials.pdf.

[61] B. Foss and T. A. N. Heirung. *Merging optimization and control*. Accessed: 2023-01-27. May 2013. URL: https://folk.ntnu.no/bjarnean/Publications/OptimalControl.pdf.

[62] J. Morales et al. *Integrating Renewables in Electricity Markets - Operational Problems*. 2014, pp. 289–330. ISBN: 9781461494119.

[63] M. Gendreau and J.Y. Potvin. *Handbook of Metaheuristics*. 2nd ed. Vol. 146. Springer, 2009.

[64] J. Kennedy and R. Eberhart. 'Particle swarm optimization'. In: *Proceedings of ICNN'95 - International Conference on Neural Networks*. Vol. 4. 1995, pp. 1942–1948.

[65] R. Storn and K. Price. 'Differential Evolution: A Simple and Efficient Adaptive Scheme for Global Optimization Over Continuous Spaces'. In: *Journal of Global Optimization* 23 (1995).

[66] K. Punyisa and J. Udom. 'A comparative study of mixed-integer linear programming and genetic algorithms for solving binary problems'. In: *2018 5th International Conference on Industrial Engineering and Applications (ICIEA)*. 2018, pp. 284–288.

[67] K. Nieminen, S. Ruuth and I. Maros. *Genetic algorithm for finding a good first integer solution for MILP*. Accessed: 2023-05-20. Apr. 2003. URL: https://www.doc.ic.ac.uk/research/technicalreports/2003/DTR03-4.pdf.

[68] Yuping Wang and Wei Ma. 'A Penalty-Based Evolutionary Algorithm for Constrained Optimization'. In: *Advances in Natural Computation*. Ed. by Licheng Jiao et al. Berlin, Heidelberg: Springer Berlin Heidelberg, 2006, pp. 740–748.

[69] K. Thorvaldsen, S. Bjarghov and H. Farahmand. 'Representing Long-term Impact of Residential Building Energy Management using Stochastic Dynamic Programming'. In: (Aug. 2020).

[70] R. Sinha et al. 'Flexibility from Electric Boiler and Thermal Storage for Multi Energy System Interaction'. In: *Energies* 13 (2019), p. 98.

[71] S. V. Pandiyan and J. Rajasekharan. 'Recursive training based physics-inspired neural network for electric water heater modeling'. In: *Energy Informatics* 5 (Aug. 2022), p. 58.

[72] F. Plaum et al. 'Aggregated demand-side energy flexibility: A comprehensive review on characterization, forecasting and market prospects'. In: *Energy Reports* 8 (2022), pp. 9344–9362.

[73] R. Ahmadiahangar et al. 'Forecasting Available Demand-Side Flexibility'. In: 2020, pp. 39–49. ISBN: 978-981-15-4626-6.

[74] M. Shad et al. 'Identification and Estimation for Electric Water Heaters in Direct Load Control Programs'. In: *IEEE Transactions on Smart Grid* 8.2 (2017), pp. 947–955.

[75] L. Paull, H. li and L. Chang. 'A novel domestic electric water heater model for a multi-objective demand side management program'. In: *Electric Power Systems Research - ELEC POWER SYST RES* 80 (2010), pp. 1446–1451.

[76] L. Ø. Öberg. *Hva skal til for at husholdningskunder blir aktive i et fleksibilitetsmarked? The Smart Grid Conference 2022, Scandic Hell Værnes*. Sept. 2022.

[77] F. Najafi and M. Fripp. 'Stochastic optimization of comfort-centered model of electrical water heater using mixed integer linear programming'. In: *Sustainable Energy Technologies and Assessments* 42 (2020).

[78] G. Shen et al. 'A Data-Driven Electric Water Heater Scheduling and Control System'. In: *Energy and Buildings* 242 (2021), p. 110924.

[79] Y. Zhaojing et al. 'Optimal Scheduling Strategy for Domestic Electric Water Heaters Based on the Temperature State Priority List'. In: *Energies* 10.9 (2010), p. 1425.

[80] P. Olivella-Rosell et al. 'Optimization problem for meeting distribution system operator requests in local flexibility markets with distributed energy resources'. In: *Applied Energy* 210 (2018), pp. 881–895.

[81] Arva AS. *SMART SENJA - fremtidens energisystem*. Accessed: 2023-02-14. URL: https://smartsenja.no/.

[82] SVK. *sthlmflex*. Accessed: 2022-11-09. Nov. 2021. URL: https://www.svk.se/sthlmflex.

[83] K. Heussen et al. 'A clearinghouse concept for distribution-level flexibility services'. In: *IEEE PES ISGT Europe 2013*. 2013, pp. 1–5.

[84] NODES. *IntraFlex: Auto-rebalancing energy suppliers*. Accessed: 2023-01-25. Nov. 2019. URL: https://nodesmarket.com/case/intraflex/.

[85] Arva AS. *NYE VARMTVANNSTANKER TIL NORD-SENJA*. Accessed: 2023-06-08. May 2023. URL: https://smartsenja.no/nye-varmtvannstanker-til-nord-senja/.

[86] P. Kepplinger, G. Huber and J. Petrasch. 'Demand Side Management via Autonomous Control-Optimization and Unidirectional Communication with Application to Resistive Hot Water Heaters'. In: *Nachhaltige Gebäude. Versorgung - Nutzung - Integration. e-nova. Internationaler Kongress 2014. 13. und 14.* Leykam, 2014.

[87] C. A. Correa-Florez, A. Michiorri and G. Kariniotakis. 'Optimal Participation of Residential Aggregators in Energy and Local Flexibility Markets'. In: *IEEE Transactions on Smart Grid* 11 (2020), pp. 1644–1656.

[88] T. Sousa et al. 'Evaluation of different initial solution algorithms to be used in the heuristics optimization to solve the energy resource scheduling in smart grids'. In: *Applied Soft Computing* 48 (2016), pp. 491–506.

[89] D. Mariano-Hernández et al. 'A review of strategies for building energy management system: Model predictive control, demand side management, optimization, and fault detect diagnosis'. In: *Journal of Building Engineering* 33 (2020), p. 101692.

[90] H. Ren et al. 'Optimal scheduling of an EV aggregator for demand response considering triple level benefits of three-parties'. In: *International Journal of Electrical Power Energy Systems* 125 (2021), p. 106447.

[91] S. Ø. Ottesen, A. Tomasgard and S. Fleten. 'Prosumer bidding and scheduling in electricity markets'. In: *Energy* 94 (2016), pp. 828–843.

[92] S. Ø. Ottesen, A. Tomasgard and S. Fleten. 'Multi market bidding strategies for demand side flexibility aggregators in electricity markets'. In: *Energy* 149 (2018), pp. 120–134.

[93] Y. Bin et al. 'Bi-level scheduling Model of Air conditioning load aggregator considering users' comfort compensation'. In: *2020 5th Asia Conference on Power and Electrical Engineering (ACPEE)*. 2020, pp. 1995–2001.

[94] S. Minniti et al. 'Development of Grid-Flexibility Services from Aggregators a Clustering Algorithm for Deploying Flexible DERs'. In: *2018 IEEE International Conference on Environment and Electrical Engineering and 2018 IEEE Industrial and Commercial Power Systems Europe (EEEIC / I&CPS Europe)* (2018), pp. 1–7.

[95] M. Ali, A. Safdarian and M. Lehtonen. 'Demand response potential of residential HVAC loads considering users preferences'. In: *IEEE PES Innovative Smart Grid Technologies, Europe*. 2014, pp. 1–6.

[96] S. Nojavan and K. Zare. *Electricity markets - new players and pricing uncertainties*. Springer Cham, 2020, pp. 199–212.

[97] L. Roald et al. 'Power systems optimization under uncertainty: A review of methods and applications'. In: *Electric Power Systems Research* 214 (2023), p. 108725.

[98] A. Amadeh, Z. E. Lee and K. M. Zhang. 'Quantifying demand flexibility of building energy systems under uncertainty'. In: *Energy* 246 (2022), p. 123291.

[99] J. Widen et al. 'Constructing load profiles for household electricity and hot water from time-use data—Modelling approach and validation'. In: *Energy and Buildings* 41.7 (2009), pp. 753–768.

[100] J. Widen and E. Wäckelgård. 'A high-resolution stochastic model of domestic activity patterns and electricity demand'. In: *Applied Energy* 87.6 (2010), pp. 1880–1892.

[101] J. Widen, E. Wäckelgård and A. Nilsson. 'A combined Markov-chain and bottom-up approach to modelling of domestic lighting demand'. In: *Energy and Buildings* 41.10 (2010), pp. 1001–1012.

[102] Nord Pool. *Regulating prices*. Accessed: 2023-05-20. URL: https://www.nordpoolgroup.com/en/Market-data1/Regulating-Power1/Regulating-Prices1/NO1/Hourly/?view=table.

[103] A. Hassanat et al. 'Choosing Mutation and Crossover Ratios for Genetic Algorithms—A Review with a New Dynamic Approach'. In: *Information* 10 (2019), p. 390.

[104] M. Andersson and D. Mellin. *Genetic Algorithms: Comparing Evolution With and Without a Simulated Annealing-inspired Selection*. Accessed: 2023-05-20. June 2019. URL: https://www.diva-portal.org/smash/get/diva2:1350811/FULLTEXT01.pdf.

[105] F. Chicano et al. 'Fitness Probability Distribution of Bit-Flip Mutation'. In: *Evolutionary computation* 23 (Sept. 2013).

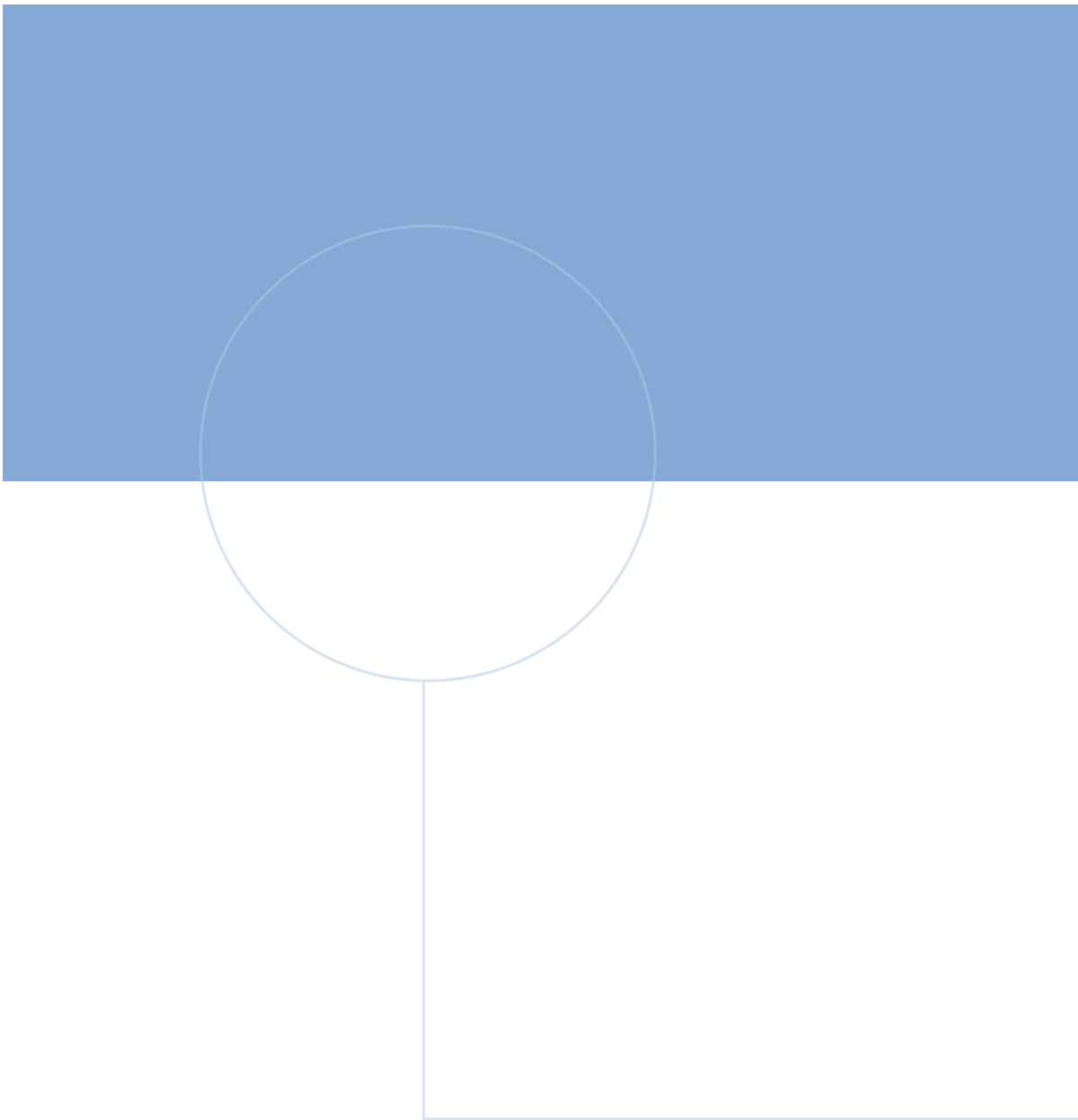

NTNU

Norwegian University of
Science and Technology